NASA Contract Report 172245

Design of Sidewall Treatment For Cabin Noise Control of a Twin Engine Turboprop Aircraft

R. Vaicaitis and M. Slazak

Modern Analysis Inc.
Ridgewood, New Jersey

CONTRACT NAS1-16117
December 1983

NASA
National Aeronautics and Space Administration

Langley Research Center
Hampton, Virginia 23665

ENTER:

DISPLAY 16/6/1

85N30771*# ISSUE 19 PAGE 3351 CATEGORY 71 RPT#: NASA-CR-172245 NAS 1.26:172245 CNT#: NAS1-16117 83/12/00 88 PAGES UNCLASSIFIED DOCUMENT

UTTL: Design of sidewall treatment of cabin noise control of a twin engine turboprop aircraft

AUTH: A/VAICAITIS, R.; B/SLAZAK, M.

CORP: Modern Analysis, Inc., Ridgewood, N. J. AVAIL.NTIS

SAP: HC A05/MF A01

CIO: UNITED STATES

MAJS: /*ACOUSTIC RETROFITTING/*AIRCRAFT COMPARTMENTS/*AIRCRAFT NOISE/*NOISE PREDICTION (AIRCRAFT)/*NOISE PROPAGATION/*NOISE REDUCTION

MINS: / ALUMINUM/ FOAMS/ HONEYCOMB STRUCTURES/ MATHEMATICAL MODELS/ OPTIMIZATION / PANELS/ POROUS MATERIALS

ABA: R.J.F.

NASA Contract Report 172245

Design of Sidewall Treatment For Cabin Noise Control of a Twin Engine Turboprop Aircraft

R. Vaicaitis and M. Slazak

Modern Analysis Inc.
Ridgewood, New Jersey

CONTRACT NAS1-16117
December 1983

National Aeronautics and
Space Administration

Langley Research Center
Hampton, Virginia 23665

TABLE OF CONTENTS

LIST OF TABLES

LIST OF FIGURES

1. Summary

An analytical procedure has been used to predict the noise transmission into the cabin of a twin-engine G/A aircraft. The basic concept of the theoretical model is that of modal superposition wherein the acoustic modes in the cabin and the structural modes of the sidewall panels are accounted for. This model was then used to optimize the sidewall acoustic treatment to reduce the interior A-weighted noise level to an average value of about 85 dBA.

The noise input pressure due to propeller blade passage harmonics and to turbulent surface flow is expressed in the form of a propagating random pressure field. The surface pressure noise spectral levels were selected utilizing experimental flight data and empirical predictions. The cabin interior is approximated as a rectangular enclosure. The sidewalls of the aircraft are modeled by several discretely stiffened panel units. The windows are treated as individual plexiglass panels. The finite element strip method and transfer matrix techniques are used to calculate the natural frequencies and normal modes of the stiffened panels. The modes and frequencies of the window panels are calculated utilizing closed form solutions. The additional noise losses due to multilayered sidewall treatments composed of acoustic blankets, septum, air spaces and trim, are estimated by the impedance transfer method.

The add-on treatments considered in this optimization study include aluminum honeycomb panels, constrained layer damping tape, porous acoustic blankets, acoustic foams, septum barriers and limp trim panels which are isolated from the vibration of the main sidewall structure. To reduce the average noise level in the cabin from about 102 dBA (untreated) to 85 dBA (optimized), the added weight of the noise control treatment is about 2% of the total gross take-off weight of the aircraft.

2. Introduction

The main emphasis of the present study is to optimize interior noise in a typical twin-engine G/A aircraft utilizing existing analytical methods and add-on treatments. The details of the analytical noise transmission model employed are given in [1]. The basic concept of this model is that of modal analysis wherein the acoustic modes in the cabin and the structural modes of the sidewall are accounted for. The geometry of the aircraft cabin (Fig. 1) used for this study suggests that the interior acoustic space may be treated as a rectangular enclosure. Such an idealization of the cabin allows for simple representation of the acoustic modes. However, if the acoustic modes were known for the actual shape of the cabin, the modal decomposition of the acoustic cavity would still be valid, but the numerical procedures used to estimate the noise transmission would be more involved. The sidewalls of the aircraft are modeled by several discretely stiffened panel units. The double wall windows are represented by equivalent single sheet flat plexiglass panels. The frames are included in the structural model either as discrete stiffening elements of the skin-stringer panels or as flexible elastic boundaries. The normal modes and natural frequencies of the stiffened panels are obtained utilizing the finite element strip [2,3] and transfer matrix [4,5] methods. The effect of aircraft pressurization is included when calculating the natural frequencies of the sidewall panels.

The exterior surface pressures acting on the sidewalls of the aircraft are represented by a random convecting pressure field. The noise spectral levels at several locations are determined from experimental flight data. Due to the limited amount of flight data available, the surface pressure intensity is distributed over the sidewall of the aircraft according to empiri-

cal propeller noise input predictions [6]. Furthermore, the convection trace velocities are estimated in approximation from ground and taxi tests given in [7,8].

The noise attenuation due to add-on treatments which are not attached directly to the structure are calculated using existing methods based on acoustic impedance transfer [9,10]. The multilayered add-on treatments include porous acoustic blankets, thin septum barriers, acoustic foams and soft trim panels which are isolated from the vibration of the main sidewall structure. Then, the total noise losses are obtained by combining the contributions from treatments which are directly attached to the skin (honeycomb panels and damping tape) and those treatments which are not attached to the skin (acoustic blankets, foams, septa, trim). The numerical calculations are repeated for several different values of the surface densities of the add-on treatments. Engineering judgment is exercised to limit the number of treatment combinations and the values of the add-on surface densities. Then, several treatments which are capable of reducing cabin noise to an acceptable level are selected. The one which gives the least added weight is taken as the optimized sidewall treatment.

3. Analytical Model

The basic concept of the analytical model used to calculate noise transmission into the aircraft cabin is that of modal analysis. This approach has been used for many noise transmission related problems [1,3,5,11-16]. Modal analysis seems to be an attractive and efficient method to be used for the study of low frequency noise transmission into the cabin of a propeller driven aircraft.

3.1 Acoustic Model

The interior space of the twin-engine aircraft shown in Fig. 1 is approximated by a rectangular enclosure occupying a volume V = abd. It is assumed that the main contribution to the cabin noise is due to the airborne noise transmitted by the sidewalls at z = 0, d (shown by crossed lines in Fig. 2), and that the remaining surfaces are acoustically rigid (noise transmission through these surfaces is assumed to be small). Such an assumption seems to be justified due to the very stiff floor and ceiling construction and their greater distance from the propeller tips (Fig. 1). Furthermore, noise entering through the windshield and forward and aft bulkheads is also assumed to be negligible when compared to the noise transmitted through the sidewalls. The contribution to noise losses due to interior absorption (treated walls and ceiling, seats, passengers, carpeting) is included in the analytical model as an "equivalent" acoustic damping.

The solution for the acoustic pressure, p, inside the enclosure has been developed in the form of the spectral density $S_p(x,y,z,\omega)$ [1,5]. The sound pressure levels in the cabin are then obtained from

$$SPL(x,y,z,\omega) = 10 \log \{S_p(x,y,z,\omega)\Delta\omega/p_0^2\} \qquad (1)$$

where $\Delta\omega$ is the selected bandwidth and p_0 is the reference pressure (p_0 = 2.9 x 10^{-9} psi, p_0 = 20μN/m^2). The interior noise levels given by Eq. 1 correspond to the noise transmitted by a single stiffened panel unit or window unit located at either z = 0 or z = d. The total noise transmitted by all the panel units composing the entire sidewall is determined by superposition of the sound pressure contributions from all the flexible panels. Such a superposition is only valid if the response of each panel unit is taken to be independent.

3.2 Structural Model

The sidewalls of the baseline aircraft shown in Fig. 1 are composed of an external skin which is stiffened by frames and several single- and double-wall window units. The structural model selected for the present study is shown in Fig. 3 where the sidewall is segmented into four stiffened skin-stringer panels, two single panels, and six windows. The amount of noise transmitted through other surfaces of the sidewall is assumed to be small. Such a segmentation offers significant advantages for noise transmission path identification and computational simplification. Such an idealization seems to be justified for this type of aircraft construction due to the very stiff boundary conditions provided by the frames. The treated aircraft interior includes porous blankets for thermal and acoustic insulation, septum barriers and trim panels. The solution for the acoustic pressure given in Eq. 1 is a function of the response of each of the panel units shown in Fig. 3. Assuming that the acoustic blankets, septum barriers and trim panels have no direct effect on the vibration of the elastic panels, the response of these panels due to propeller noise and turbulent boundary layer inputs can be developed in a straightforward fashion utilizing a modal expansion procedure [1,5]. The solu-

tion is ultimately expressed in the form of the spectral density of the panel deflection response $S_w^i(x,y,\omega)$ where the superscript i indicates the i-th panel unit shown in Fig. 3. To complete the solution for panel deflections and subsequently for the cabin noise pressure, the natural frequencies and normal modes of the flexible panels need to be known.

3.3 Natural Frequencies and Normal Modes of Sidewall Panels

3.3.1 Single panels

In addition to the stiffened panel units (Nos. 9,10,11 and 12), the aircraft sidewall contains two single panels (Nos. 4 and 6) and six windows (Nos. 1,2,3,5,7 and 8). The port side pilot window (No. 1) is a single sheet curved panel while all other windows are of double wall construction. In the present study, the double wall windows are replaced with single sheet flat panels which are taken to be simply supported on all four edges. Furthermore, the slightly irregular window shapes are approximated by rectangular panels. The elastic aluminum panels Nos. 4 and 6 are also assumed to be simply supported on all four edges. Then, the natural frequencies are calculated from

$$f_{mn} = \tfrac{1}{2}\{D\pi^2(m^2/L_x^2 + n^2/L_y^2)/\overline{\rho h} + (N_x m^2/L_x^2 + N_y n^2/L_y^2)/\overline{\rho h}\}^{\frac{1}{2}} \qquad (2)$$

where D is plate stiffness and N_x and N_y are the in-plane force resultants arising from pressurization of the cabin. For a cylindrical fuselage, the in-plane forces can be expressed as

$$N_x = \Delta pR/2 \qquad (3)$$

$$N_y = \Delta pR \qquad (4)$$

where Δp is the pressure differential and R is the radius of the fuselage. From Fig. 1, it can be seen that the curvature of the aircraft selected in this study changes along the periphery. Thus, the in-plane loads are calculated from Eqs. 3 and 4 in approximation by selecting an average value for

the radius R. The normal modes for these simply supported panels are

$$X_{mn}(x,y) = \sin\{(m\pi/L_x)(x-a_0)\} \sin\{(n\pi/L_y(y-b_0)\} \quad (5)$$

where a_0 and b_0 are the distances from the x and y axes, respectively, to the panel location.

3.3.2 Discretely stiffened panels

Here we seek the natural frequencies and normal modes of two-dimensional panels which are discretely stiffened by frames (Nos. 9,10,11 and 12) as shown in Fig. 3. The frames are thin wall members of an open cross-section as shown in Fig. 4. The Type 1 frame is the main stiffening ring of the fuselage construction. The cross-sectional shape of this frame (given in Fig. 4) is an idealization of a complex configuration wherein the straps are composed of two layers which vary nonuniformly along the periphery and extend only over a portion of the ring. The geometric and section properties of these constructions were calculated by dividing the cross-sectional shape into a number of sub-elements and then using the general theory of thin-walled open sections [17,18]. These results are presented in Table 1.

The natural frequencies, f_{mn}, and normal modes, X_{mn}, of these stiffened panels were determined by using the finite element strip [2,3] and/or transfer matrix [1,4,5] methods. The finite element strip method could provide computational advantages over the transfer matrix approach for those cases where the number of panel bays is large, the distances between the stiffening elements are uneven and the stiffness of the frames is large. A detailed description of the transfer matrix procedure can be found in [4]. A brief description of the finite element strip method will now be given.

The finite element strip method developed in [2] has been used very efficiently to analyze two dimensional structures for which the modal solutions

can be prescribed in one direction. This method has been extended for noise transmission applications through curved skin-stringer panels [3]. The skin-stringer panels shown in Fig. 3 are assumed to be simply supported along the frames at $y = b_0$ and $y = b_0 + L_Y$. The eigenfunctions $\psi_n(y)$ of the panel corresponding to the y-coordinate are taken to be beam functions which satisfy the given boundary conditions at the frames. The skin-stringer panel is divided into a number of flat strip elements. Each stringer (frame) is taken as an element which is compatible with the bounding strip element of the plate. Then, following the procedure presented in [2,3], the stiffness (K_{mn}) and mass (M_{mn}) matrices of the strip element are determined. To estimate the stiffness and mass matrices of each stringer, an existing theory which deals with an average thin-walled member of an open cross-section [17,18] is used. Point O indicates a position through which moment and shear loads are transferred between the skin and stiffener. For the constructions shown in Fig. 4, point O is taken as the mid-point of the total contact between the skin and the flanges of the stiffener. Furthermore, the reference co-ordinates (x,z) are taken through this point. The symbol C'denotes the location of the centroid. Assuming that the shear strains on the x-z plane are negligible and that the plane sections remain normal to the middle surface after deformation, the expressions for the strain and kinetic energy of the stiffener can be determined [3]. Defining the nodal displacement matrix $\{\delta_n\}$ as a base vector, the total energy (strain + kinetic) of a skin-stringer panel can be expressed as

$$E = \tfrac{1}{2} \sum_{n=1}^{r} (\{\delta_n\}^T [K_n] \{\delta_n\} + \omega^2 \{\delta_n\}^T [M_n] \{\delta_n\}) \qquad (6)$$

where K_n and M_n are the banded stiffness and mass matrices, res-

pectively, r is the total number of modes along the y-coordinate and the superscript T indicates matrix transposition. These global matrices are constructed using the nodal stiffness and nodal mass matrices of the panel strip elements and stringers [3]. Minimizing the total energy E with respect to the nodal displacements $\{\delta_m\}$ by setting $\partial E/\partial\{\delta_m\} = 0$, we obtain the characteristic equation

$$[K_m] - \omega^2[M_m] = 0 \tag{7}$$

The eigenvalues of this equation are the natural frequencies and the eigenvectors are the corresponding normal modes X_{mn} of the skin-stringer panel. The solutions to Eq. 7 are obtained using standard available computer codes for eigenvalue problems.

3.4 External Pressure Field

The external surface pressure acting on the aircraft is propeller noise due to the blade passage harmonics and turbulent boundary layer. The cross-spectral density of the input pressure is assumed to be separable in the direction of propagation and that perpendicular to it and is given as

$$S_j^e(\xi,\eta,\omega) = S_j(\omega)\, e^{i\omega\xi/V_x}\, e^{i\omega\eta/V_y} \tag{8}$$

where $S_j(\omega)$ is the power spectral density for the j-th panel unit, $\xi = x_2 - x_1$, $\eta = y_2 - y_1$ are the spatial separations, and V_x and V_y are the trace velocities corresponding to the x- and y-directions, respectively. The expression given in Eq. 8 is limited to spatially non-decaying convecting sound pressure fields. The sound pressure levels characterized by the spectral density $S_j(\omega)$ are taken to be uniformly distributed over each panel surface,

but varying in a step-wise fashion from one panel to another. These spectral densities are obtained from the exterior surface pressure data measured in flight. In addition, the empirical prediction of surface noise due to propeller blade passage harmonics are utilized to distribute the noise intensities over the aircraft fuselage [6]. Subsonic trace velocities corresponding to the propeller rotation tip speed were taken for the vertical direction y, and sonic trace velocities were assumed for the longitudinal direction x (normal to the propeller rotation plane). The values of V_y = 510 ft/sec and V_x = 1100 ft/sec were used for all numerical computations.

The exterior sound pressure levels acting on Panel No. 1 are shown in Fig. 5. The base level of about 99 dB is mainly due to surface flow resulting from the turbulent boundary layer. The turbulent boundary layer noise is taken to be fully correlated and uniformly distributed over the panel surface. These results correspond to cruise conditions at an altitude of 15,000 ft. The input noise levels for the twelve panel units shown in Fig. 3 are given in Table 2 where the SPL (sound pressure levels) at each blade passage harmonic and the base levels are given. The base levels are selected to represent turbulent boundary layer pressure for each panel units. These results are then converted to spectral densities S_i utilizing a 2.5 Hz bandwidth.

4. Noise Attenuation Due to Add-On Treatments

The analytical model described in Section 3 predicts noise transmission for the baseline aircraft without add-on treatments. The add-on treatments can be divided into two basic categories. In the first case, the treatments are attached directly to the skin (honeycomb panels, damping tapes, nonload carrying mass) and have a marked influence on the structural dynamic characteristics of the panels of which the aircraft sidewall is constructed. The noise attenuation due to these treatments is estimated in the same fashion as that described in Sec. 3, but the natural frequencies, normal modes and generalized mass are calculated by including the effect of the add-on treatment. In the second case, the treatments are not attached directly to the skin (acoustic blankets, foams, septum barriers, trim panels) and it is assumed they have no significant influence on the vibration of the sidewall panels. The noise attenuation of these treatments is calculated by a separate procedure described in Sec. 4.2.

4.1 Noise Losses Due to Honeycomb Panel and Damping Tape Treatments

Additional stiffening can be achieved by attaching honeycomb panels to the interior walls of the aircraft as shown in the sketch below:

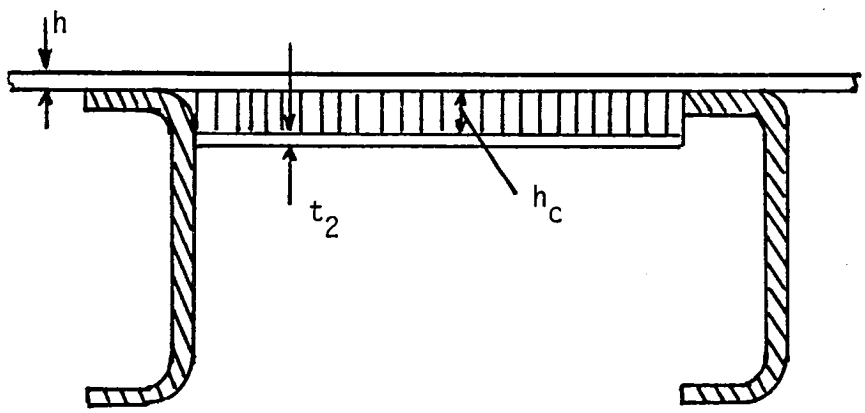

The transverse stiffness of the treated panel (elastic skin + honeycomb + facing) can be obtained from

$$D_h = \frac{E_1 E_2 t_1 t_2 h_c^2}{(E_1 t_1 + E_2 t_2)(1 - \nu^2)} \tag{9}$$

where h_c is the distance between the facing centroids, ν is Poisson's ratio of the facings ($\nu_1=\nu_2=\nu$), E_1, E_2 and t_1, t_2 are the effective moduli and thicknesses of the skin panel and honeycomb facing, respectively. Due to the practical difficulties of attaching a two-face honeycomb panel to a curved surface, a honeycomb construction with only one facing is considered in this study. After the attachment of this honeycomb panel to the aircraft skin, the skin panel acts as a facing to the honeycomb construction.

Due to the significant increase in the total treated panel stiffness (aluminum panel + honeycomb panel), the modal frequencies of these panels shift to higher frequency values. The stiffening effect is included by replacing the plate stiffness D in Eq. 2 by the combined stiffness D_h given in Eq. 9 when calculating the modal frequencies for single panels which are simply supported on all edges. The increase in surface density due to honeycomb treatment is accounted for by replacing the $\bar{\rho}h$ value in Eq. 2 by a value corresponding to that of a treated panel. The natural frequencies and normal modes of the skin-stringer panels stiffened by honeycomb panels are calculated following the procedures presented in Sec. 3.3.2 but with the panel stiffness and surface density adjusted according to the amount of honeycomb treatment.

The additional noise losses due to honeycomb treatment are obtained by subtracting the sound pressure levels of the treated case from that of the

untreated. The interior sound pressure levels in both of these cases are calculated according to the procedures described in Sec. 3.

Predicting the actual noise losses that will result from damping treatments in a particular system is a difficult task. The greatest uncertainty is usually in estimating the damping of a structure as a function of frequency. In the present study, a constrained layer damping tape that is especially effective for low frequencies and low temperatures is considered. The modal structural damping coefficient of a panel treated with constrained layer damping tape is taken as

$$\zeta_{mn} = (\zeta_p + \zeta_T)(\omega_{11}/\omega_{mn}) \tag{10}$$

where ζ_p is the damping coefficient corresponding to a skin-stringer panel, ζ_T is the additional damping due to damping tape treatment and ω_{mn} are the modal frequencies. Experimental data [19] indicate values for ζ_p on the order of 0.01 - 0.015 for untreated skin-stringer panels and 0.02 - 0.03 for panels stiffened with honeycomb panels. The damping coefficient ζ_T is calculated using the procedures of constrained layer damping presented in Ref. 20. Typical values for ζ_T are 0.025 for one layer treatment and 0.05 for two layer treatment. When damping tape is added to a panel surface, the mass of the panel increases, without an appreciable increase in the panel stiffness. Thus, the modal frequencies of the treated panels tend to shift to the lower frequency values. This effect is accounted for by replacing the surface density and generalized mass of the panels by ones corresponding to the damping tape treatment. The effect on noise transmission due to the addition of damping tape is estimated from the analytical model given in Sec. 3.

To estimate the noise attenuation due to an increase in stiffness, mass and damping, the analytical noise transmission prediction model described in Sec. 3 is used. However, it is useful to establish simple guidelines for a preliminary estimation of the noise attenuation due to add-on treatments which are directly attached to the aircraft skin. The sound pressure spectral density inside the cabin for each structural mode is proportional to

$$S_p \sim \frac{S(\omega)}{M_{mn}^2[(\omega_{mn}^2 - \omega^2)^2 + 4\zeta_{mn}^2\omega_{mn}^2\omega^2]} \cdot A_c \tag{11}$$

where $S(\omega)$ = the input spectral density, M_{mn} = generalized mass, ω_{mn} = natural frequencies, ζ_{mn} = modal damping coefficients, A_c = acoustic terms. The sound pressure levels in the cabin are calculated from

$$\Delta TL = 10 \log(S_p \Delta\omega / p_0) \tag{12}$$

where $\Delta\omega$ = bandwidth, p_0 = reference pressure. Then, the change in the sound pressure levels can be estimated from

$$\Delta SPL = 10 \log(S_p^U / S_p^T) \tag{13}$$

where S_p^U = pressure spectral density for the untreated structure, S_p^T = pressure spectral density for the treated structure.

At the resonance of each structural mode, Eq. 11 reduces to

$$S_p \sim \frac{S(\omega_{mn})}{4M_{mn}^2\zeta_{mn}^2\omega_{mn}^4} \cdot A_c \tag{14}$$

For the frequencies away from the resonance condition,

$$S_p \sim \frac{S(\omega)}{M_{mn}^2\omega^4} \cdot A_c \tag{15}$$

Then, from Eqs. 13-15,

$$\Delta TL\Big|_{\text{at resonance}} \doteq 10 \log \left(\frac{M_{mn}^T \zeta_{mn}^T \omega_{mn}^{T^2}}{M_{mn}\zeta_{mn}\omega_{mn}^2}\right)^2 \tag{16}$$

$$\Delta TL\Big|_{\text{off resonance}} \doteq 10 \log \left(M_{mn}^T/M_{mn}\right)^2 \tag{17}$$

where the superscript T indicates a treated case. For the orthogonal panel modes considered in this study, the generalized mass is $M_{mn} = m_p L_x L_y/4$ where m_p is the panel mass per unit area, and L_x, L_y are the panel dimensions. From Eqs. 10, 16 and 17

$$\Delta TL\Big|_{\text{at resonance}} \doteq 10 \log \left(\frac{m_p^T(\zeta_p + \zeta_T)\omega_{11}^T \omega_{mn}^T}{m_p \zeta_p \omega_{11}\omega_{mn}}\right)^2 \tag{18}$$

$$\Delta TL_{\text{off resonance}} \doteq 10 \log \left(m_p^T/m_p\right)^2 \tag{19}$$

In obtaining Eqs. 18 and 19, it was assumed that the mode shapes of the panels are the same for both treated and untreated cases. The effect of acoustic modal resonances are not included. Furthermore, ΔTL is calculated at and off resonance and the contributions from other modes at that frequency are not included (i.e., the modes are not summed). Thus, these equations should be viewed as approximate guidelines for estimating the additional noise reduction due to add-on treatments attached directly to the skin.

4.2 Additional Noise Losses Due to Acoustic Blankets, Acoustic Foams, Septum Barriers and Trim Panels

The added transmission losses ΔTL have been calculated for the multilayered wall construction shown in Fig. 6. Following the procedure presented in [1, 9-11], the ΔTL at an incident plane wave angle θ_1 is obtained from

$$\Delta TL(\omega,\theta_1) = 10 \log \left| \frac{(p_1/p_2)_{untreated}}{(p_1/p_2) \cdots (p_{n-1}/p_n)_{treated}} \right|^2 \qquad (20)$$

where p_{n-1}/p_n are the pressure ratios across the boundaries between adjacent media and the pressure ratio across the media themselves as shown in Fig. 6. Acoustic plane waves are incident on the exterior of the sidewall with an angle θ_1 and transmitted according to the various impedances present for each different layer. The interior of the medium is assumed to extend to infinity with an acoustic termination impedance ρc. Numerical results were obtained for treatments composed of up to nine layers, including the elastic skin-stringer panel. The treatment layers are composed of acoustic blankets or acoustic foams and septum barriers. The impedances for the acoustic blankets were calculated from the relations given in [9] while for the acoustic foams empirical expressions were used [10,21]. In the latter case, the propagation constant through a porous layer is expressed as

$$\lambda = \alpha + i\beta \qquad (21)$$

where the empirical relations suggested in [10] for α and β are

$$\alpha = (\omega/c)\ [0.189(\rho\omega/2\pi R_1)^{-0.595}] \qquad (22)$$

$$\beta = (\omega/c)\ [1 + 0.978(\rho\omega/2\pi R_1)^{-0.700}] \qquad (23)$$

where c is the speed of sound in the gas of the porous material, ρ is the density of the gas and R_1 is the flow resistivity of the porous material. In general, the ratio $\rho\omega/2\pi R_1$ for porous materials is limited to ($0.01 \leq \rho\omega/2\pi R_1 \leq 1$). However, Bies and Hansen [21] have recently extended the empirical relations for α and β to values of $\rho\omega/2\pi R_1$ much less than

0.01. Thus, a closed cell foam could exhibit the behavior of a semi-rigid material resulting in a much higher flow resistivity R_1 than that of the commonly used acoustic blankets. Under such conditions, a significant amount of noise attenuation might be realized even for the low frequency range where the noise intensity due to propeller blade passage harmonics is the highest. However, the data on such foam materials is limited and more theoretical and experimental work is needed on this subject.

The interior noise levels in a completely treated cabin are calculated from

$$SPL(x,y,z,\omega)\Big|_{treated} = SPL(x,y,z,\omega)\Big|_{untreated} - \Delta TL_1(\omega) - \Delta TL_2(\omega) \tag{24}$$

where ΔTL_1 are the noise losses due to treatments which are directly attached to the aircraft skin and ΔTL_2 are the additional noise losses due to all other treatments including the absorption effects in the cabin.

5. Interior Noise Optimization

The procedures described in previous sections are used to optimize the cabin noise in a twin engine G/A aircraft to an average overall A-weighted level of about 85 dBA. To achieve this goal, the following add-on treatments were selected: lightweight aluminum honeycomb panels, constrained layer damping tapes, porous acoustic blankets, thin layers of septum barriers, acoustic foams, and limp trim panels which are isolated from the vibration of the main sidewall structure. In the optimization procedure, an interior point in the cabin, located in the propeller plane at about ear level and eight inches from the sidewall, was selected. The interior noise was estimated at this point for various add-on treatment conditions. The noise transmitted by each panel unit (Fig. 3) was calculated for each add-on treatment and for combinations of these treatments. Numerical computations were performed using a narrow band analysis for a bandwidth of $\Delta f = 2$ Hz and frequency range from 0 - 1122 Hz. The optimization criteria were based on the A-weighted one-third octave noise levels which were calculated from the narrow band results. A more detailed description of the optimization procedure is given in Ref. 1.

6. Numerical Results

6.1 Modes and Frequencies

6.1.1 Baseline and Honeycomb Stiffened Panels

The normal modes and natural frequencies were obtained using the finite element strip method and the transfer matrix procedures described in Section 3.3. The frequencies of the windows were determined using Eq. 2. The modes of these panels are the sine modes corresponding to simple support boundary conditions. The stiffened panel and frame geometries are shown in Figs. 3 and 4. The skin of all the aluminum panels has a thickness of 0.063 inches while the windows (each sheet) are made from 0.25 inch thick plexiglass. The geometric and material properties of the stiffeners and panels are given in Tables 1 and 3, respectively. Utilizing these data, the natural frequencies and normal modes were calculated for all the panels shown in Fig. 3 for both treated and untreated cases.

The natural frequencies corresponding to baseline panels are given in Table 4. Due to the large number of natural frequencies for the selected frequency range (1122 Hz), only the first six modal frequencies are included in this table. The frequencies and modes for the stiffened panels (Nos. 9, 10, 11 and 12) were calculated utilizing the finite element strip method. Simple support boundary conditions were assumed at the extreme edges of all the panels. Several typical mode shapes for the stiffened panel unit No. 11 are shown in Fig. 7 .

The natural frequencies and normal modes of the sidewall panels stiffened with honeycomb panels were calculated using Eqs. 2 and 9 for single panels (Nos. 4 and 6) and the transfer matrix method for skin-stringer panels (Nos. 9, 10, 11 and 12). The structural dynamic characteristics of the treated

skin-stringer panels were estimated from Eq. 9 and the stiffener properties are given in Table 1. The natural frequencies of the sidewall panels treated with honeycomb panels are presented in Table 5. The typical mode shapes of a treated skin-stringer panel are shown in Fig. 8. Due to a large increase in the structural stiffness, the modal frequencies shift to higher frequency values when compared to the results given for the baseline panels. The largest increase in modal frequency is for single panels which are supported by very stiff frames (panel Nos. 4 and 6). For the skin-stringer panels, the dynamic interaction between the stiffeners and treated skin (aluminum skin + honeycomb) is more complex. The addition of honeycomb increases the stiffness of the skin to a value which is near that of the stiffness of the intermediate stiffener. In this case, the skin-stringer panel tends to behave as a single panel unit rather than as a discretely stiffened panel. A significant amount of deflection is observed at the intermediate stiffeners and the supporting elastic boundaries. Thus, increasing the stiffness of the honeycomb treatment does not increase the modal frequencies of the skin-stringer panels by the same magnitude as that observed for single panel units.

6.1.2 Damping Tape and Mass Addition

When damping tape is added to the panel surface, the mass of the panel increases, without an appreciable increase in the panel stiffness. A similar effect is observed when a non-load carrying mass is added to the elastic panel. Thus, the modal frequencies shift to lower frequency values. For single panels, this frequency shift can be adjusted through the surface density ρh as given in Eq. 2. For skin-stringer panels, mass is added to the skin panels, with no mass added to the stringers. Thus, the modal frequencies need to be estimated using either the finite element strip or transfer matrix meth-

thods. However, it was observed that reasonable approximations can be obtained by scaling the frequencies according to

$$f_{mn}^{T} \doteq \sqrt{m/m^{T}}\ f_{mn} \qquad (25)$$

where f_{mn} are the modal frequencies in Hz, m is the mass per unit area of the panel and the superscript T indicates a treated condition. The surface density of a typical damping tape is about 0.25 lb/ft^2, while the surface density of an aircraft skin panel is 0.91 lb/ft^2. Thus, the surface density of the aircraft skin would increase by about 30% and 60% with one and two layers of damping tape added, respectively. It should be noted that such an increase in surface density corresponds only to the skin and not to the entire aircraft sidewall which is composed of skin, stiffeners, frames, straps, windows, etc. The average surface density of the entire sidewall is about 2.8 lb/ft^2. The natural frequencies calculated by the transfer matrix method are shown in Table 6 for several mass add-on treatments. These results correspond to unpressurized two, three and four span skin-stringer panels which are typical of the sidewall construction shown in Fig. 3. The frequencies given in Table 6 correspond to the first spanwise bending mode (n = 1) and the first three frequency bands of the streamwise modes. With increasing added weight, more modal frequencies will fall within the selected frequency range.

6.2 Noise Transmission Into the Aircraft

6.2.1 Baseline Aircraft: Theory and Experiment

The aircraft selected in the present study is a twin engine pressurized G/A aircraft, as shown in Fig. 1. This aircraft has a take-off gross weight of about 11,200 lbs (5,080 kg), and cruises at an airspeed of 348 mph (559

km/hr) at an altitude of 18,000 ft (486 m). The two turboprop engines are rated at 820 hp with 1591 rpm at 100% power. The propeller is three-bladed with a diameter of 8.83 ft. The cabin provides seats for pilot, co-pilot and five passengers. The flight tests for the baseline aircraft run at altitudes of 16,000 ft and 29,000 ft indicate that the A-weighted overall interior noise level varies in the cabin in the range of about 4 dBA and 8 dBA, respectively. These results correspond to Maximum Continuous Power and a 96% rpm setting. The highest interior noise levels occur in the vicinity of the propeller rotation plane. Furthermore, the highest A-weighted noise levels are in the frequency range of about 100 - 400 Hz.

The baseline aircraft to which the analytical noise transmission model is applied [1] is assumed to be an aircraft similar to the one described but with no interior treatments, although seats were left intact during the tests. The interior sound pressure levels are calculated at x = 78 in, y = 36 in, and z = 8 in (Fig. 3). The exterior sound pressure inputs corresponding to the flight conditions described in Sec. 3.4 are used. The one-third octave A-weighted interior noise levels are given in Fig. 9. The sound pressure levels presented in this report are relative values. A direct comparison between theory and the experiment is presented in Fig. 9. As can be observed from these results, the agreement between theory and experiment is relatively good. Theory seems to predict higher noise levels by about 9 dBA at the second blade passage harmonic frequency, 150 Hz. The limitations of the analytical model with regard to the uniform noise pressure distributions and to the independent responses of each panel unit are that it could overestimate the transmitted noise levels at some frequencies. Furthermore, for untreated cabins, the sound that is radiated out through the vibration of the sidewall panels might be significant. In the present model, only the panels

through which noise is being transmitted are taken to be flexible. The results tend to indicate that interior noise in the untreated aircraft is dominated by the noise transmitted through panel Nos. 4,9,10 and 11. The highest noise levels are at the second and third blade passage harmonic (fundamental blade passage harmonic = 75 Hz). The results given in Fig. 9 correspond to a structural modal damping $\zeta_p = 0.02$ and acoustic modal damping in the cabin $\xi_0 = 0.03$. The acoustic modal damping in the interior is estimated from $\xi_{ij} = \xi_0(\omega_{10}/\omega_{ij})$ where ξ_0 is the equivalent prescribed damping coefficient of the lowest acoustic mode and ω_{ij} are the modal acoustic frequencies corresponding to the x and y coordinates, respectively (Fig. 3).

6.2.2 Treated Aircraft: Theory and Experiment

The interior noise levels corresponding to light and heavy add-on treatments are calculated and then measured in flight. The flight conditions are the same as those described in Sec. 6.2.1. The light treatment is composed of two-inch thick AA fiberglass blankets. The theoretical results were obtained by first calculating the noise transmission into the bare fuselage (baseline structure) and then adding the ΔTL correction due to the fiberglass treatment. To account for the fiberglass treatment, the acoustic damping in the cabin was increased to $\xi_0 = 0.05$. The ΔTL correction was obtained utilizing the impedance transfer method described in Sec. 4.2. The theoretical and experimental interior noise levels for the aircraft treated with two-inch thick fiberglass blankets are given in Fig. 10. As can be seen from these results, the agreement between theory and experiment is relatively good. The main contribution to noise attenuation due to fiberglass blanket treatment is seen at higher frequencies (above 300 Hz).

The interior noise levels for an aircraft treated with a heavy sound-

proofing package are given in Fig. 11. A typical cross-section of the multilayered treatment and the distribution of the treatment over the sidewall are shown in Figs. 12 and 13, respectively. These results indicate a reasonably good agreement between theory and experiment. The additional noise losses ΔTL due to the treatments shown in Figs. 12 and 13 were calculated using the impedance transfer method [9]. These add-on treatments seem to be very effective in reducing the cabin noise for frequencies above 300 Hz. However, for frequencies below 300 Hz these multilayered treatments do not seem to provide the required amount of noise attenuation.

The amount of noise transmitted through the windows is relatively high for this aircraft. These estimates are based on a simple single sheet plexiglass analytical model. If the absorption in the cabin is very low (baseline structure), the sound coming through the window reverberates in the interior and the transmitted noise levels are almost the same at some distant position from the window as they are at the window. However, with a large amount of interior absorption in a treated cabin, the sound transmitted through the window is absorbed before it can travel any significant distance. In obtaining the theoretical results shown in Fig. 11, such an effect was estimated only in approximation. Experimental results tend to indicate that the increase in noise reduction due to interior absorption for the window units is about 1, 2, 3, 3, 4, 5, 6, 7, 11 and 14 dB at the one-third octave center frequencies 125, 160, 200, 250, 315, 400, 500, 630, 800 and 1000 Hz, respectively. At frequencies below 125 Hz, the effect of absorption on noise transmission seems to be negligible. However, these values should be viewed as approximate and based on limited experimental data. The contribution to cabin noise by all the windows is shown in Fig. 14.

These results indicate that in a treated cabin, the noise transmitted through windows is significant for frequencies above 300 Hz. Thus, additional add-on treatment of the metallic panels might not result in a substantial improvement in the interior noise environment for frequencies above 300 Hz.

6.3 Sidewall Treatment with Honeycomb Panels

To estimate the effect of panel stiffening, the transmitted noise was calculated for several add-on treatments composed of honeycomb constructions. Numerical results were obtained for $E_1 = E_2 = 10.0 \times 10^6$ psi, $\nu = 0.3$, $t_1 =$ 0.063 in, $h_c = 0.25$ in, $t_2 = 0.016$ in, 0.032 in and 0.063 in. The one-third octave A-weighted noise levels transmitted through the entire sidewall both with and without the honeycomb treatments are shown in Fig. 15. About 6 - 8 dBA additional noise reduction is achieved at the first three propeller blade passage harmonics with a light honeycomb treatment ($t_2 = 0.16$ in, add-on surface density $\doteq 0.25$ lb/ft^2). The gains at frequencies above 400 Hz are relatively small. Furthermore, increasing the stiffness of the honeycomb panels from $t_2 = 0.016$ in. to $t_2 = 0.032$ in. and $t_2 = 0.063$ in. results in only moderate gains in noise reduction when compared to those shown in Fig. 15. The largest amount of noise reduction due to honeycomb treatment was achieved for the single panel units (Nos. 4 and 6) which are supported with very heavy gage frames. The modal frequencies for these individual panels were calculated assuming elastic supports along the frames and rigid supports at the boundaries normal to the frames. The noise transmission through the skin-stringer panels (Nos. 9, 10, 11 and 12) treated with honeycomb do not follow the same guidelines as those of the individual panels. These differences can be attributed to the different mode shapes of these panels as described

in Sec. 6.1.1. By adding a layer of damping tape to the honeycomb panels, an additional 1 - 3 dBA noise reduction is achieved. The results presented indicate that the combination of honeycomb and damping tape treatments could provide about 7 - 8 dBA additional noise reduction in the frequency range of 70 - 300 Hz.

6.4 Sidewall Treatment with Mass and Damping Tape

The constraining damping tapes chosen in this study are composed of aluminum foil, synthetic rubber adhesive and liner. Predicting the actual noise reduction that will result from damping in a particular system is difficult. Thus, it is necessary to estimate the noise transmission for the treated and untreated panels. Several layers of damping tape can be used to achieve the proper damping requirements. The addition of damping tape also increases the surface density of the sidewall panels. The result is a higher generalized mass but lower natural vibration frequencies. Furthermore, the experiments on noise transmission for propeller driven aircraft indicate that a significant amount of the noise is transmitted not by resonance but by forced response. At the off resonance frequencies, damping tape treatment merely acts as added mass. Since the surface density of the untreated aircraft sidewall is large when compared to the surface density of the damping tape, adding one layer of damping tape would have only a small efect on noise reduction of these off resonance frequencies. However, if one of the propeller blade passage harmonics coincides with the modal frequency of a panel, damping treatment would be highly beneficial to noise reduction.

Two layers of damping tape (0.25 lb/ft^2 for one layer) and non-load carrying mass have been added to all the metallic panel surfaces shown in Fig. 3. The add-on treatment surface densities are 1 lb/ft^2 and 2 lb/ft^2.

Due to these treatments, the natural frequencies of the sidewall panels are reduced. The first three modal frequencies for both treated and untreated panels are given in Table 7. It can be observed from these results that when 2 lb/ft^2 mass is added to the aircraft skin, the panel frequencies are reduced to approximately one-half the untreated values. The damping of the untreated and treated panels was taken to be 1% and 5% of the critical damping, respectively. The noise levels transmitted through the entire sidewall (including windows) are shown in Fig. 16 with and without add-on treatments. About 6 - 8 dBA of noise reduction is achieved at the second and third blade passage harmonics. However, the noise levels increased by 5 - 13 dBA at the first blade passage harmonic. This is due to the fact that the fundamental modal frequencies of several of the sidewall panels are in the close vicinity of the first propeller blade passage harmonic. For the untreated panels, most of the fundamental frequencies are in the range of the second blade passage harmonic. As can be observed from Fig. 16, adding a large amount of mass to the aircraft skin does not produce the required noise attenuation in the low frequency range. Furthermore, for frequencies above 400 Hz, the amount of noise transmitted through windows is about the same as that transmitted through treated panels. Thus, only small gains in noise reduction are realized for frequencies above 400 Hz with mass add-on treatments.

6.5 Additional Noise Losses Due to Acoustic Blankets, Foams, Septum Barriers and Trim Panels

The additional noise losses ΔTL are calculated for a variety of multi-layered treatments using the procedures described in Sec. 4.2 and Ref. 1. Numerical results were obtained for the following data: $\eta = 0.04$, $c_1 = 1054$ ft/sec, $c_2 = c_4 = c_6 = c_8 = c_{10} = 1102$ ft/sec, $D_x = 1.7 \times 10^5$ lb_m-ft^2/sec^2, $D_y = 1.728 \times 10^6$ lb_m-ft^2/sec^2, $\rho_1 = 0.043$ lb_m/ft^3, $\rho_2 = \rho_4 = \rho_6 = \rho_8 = \rho_{10}$

= 0.068 lb_m/ft^3, ρ_m = 0.864 lb_m/ft^3, ρ_f = 21.55 lb_m/ft^3, $K_2 = K_4 = K_6 = K_8$ = 2117 lb/ft^2.

The spaces denoted by d_2, d_4, d_6 and d_8 are filled with acoustic porous blankets (AA or B type) or acoustic foams. The acoustic foams with closed cells could have larger values of the flow resistivity coefficient R_1 than do those of the acoustic blankets. The surface density μ_1 denotes the total average surface density of the sidewall which includes the aircraft skin, frames, straps, windows, etc. The surface densities μ_3, μ_5 and μ_7 correspond to the various septum barriers which separate the different layers of acoustic blankets or acoustic foams. The surface density μ_9 denotes a trim panel which is assumed to be isolated from the vibrations of the main aircraft structure.

The effect on noise losses due to different locations of the septum barriers is illustrated in Figs. 17 and 18. It can be observed that significant gains can be achieved by locating the acoustic barrier at a greater distance from the exterior elastic panel. It should be noted that the added weight does not change when the septum is placed at a different position. For the frequency range 125 - 350 Hz, the additional noise losses could range from 0 - 10 dB and 4 - 15 dB for medium weight (0.358 lb/ft^2) and heavy weight (1 lb/ft^2) septum barriers, respectively. The ΔTL is plotted in Fig. 19 for multi-layered septum combinations. For comparison, the results of a single layer barrier placed at the trim panel location are included in this figure. These results indicate that in the frequency range of 50 - 500 Hz, the multi-layered treatment is not beneficial to noise transmission control. This is mainly due to the double wall resonances of the multi-layered construction. The effect of different trim panel surface densities on ΔTL is shown in Fig. 20. These results indicate that a heavy trim panel is only beneficial for frequencies above 160 Hz. The additional noise losses corresponding

to different cavity depths, very light septum barriers and light trim are shown in Fig. 21. The total cavity depth is taken to be $d = d_2 + d_4 + d_6 + d_8$ where $d_2 = d_4 = d_6 = d_8$. A significant amount of noise attenuation can be realized for deep cavities. Furthermore, as the distance between the elastic panel and the trim panel increases, the double wall resonance frequency decreases [10]. The maximum possible distance d for the aircraft considered in this study is about 4 inches. Typical distances between the exterior panel and the trim panel of this aircraft range from about 2 inches to 3.2 inches. Thus, by increasing the treated space to 4 inches or more, an addition 3-5 dBA noise reduction might be achieved in the frequency range of 100 - 400 Hz.

The additional noise losses achieved by acoustic blankets and acoustic foams are shown in Fig. 22 for different values of the flow resistivity coefficient R_1. The flow resistivity of acoustic blankets ranges up to about 4.5 x 10^4 mks ryal/m. The results given in Fig. 22 for R_1's larger than 4.5 x 10^4 mks ryal/m correspond to semi-rigid materials. A closed cell acoustic foam could exhibit noise transmission characteristics similar to those of semi-rigid material. As can be observed from these results, significant noise transmission losses can be obtained using materials with a large value of flow resistivity. However, the experimental data needed to estimate the acoustic properties of these materials is limited. Furthermore, for large values of R_1 the ratio $\rho\omega/2\pi R_1$ would exceed the limiting range of the applicability of this theory (Sec. 4.2). Thus, the results presented in Fig. 22 should be viewed as preliminary guidelines. The effect on ΔTL of a multilayered treatment composed of materials with different flow resistivities is illustrated in Fig. 23. By placing the lighter materials near the elastic panel and the heavier materials near the trim panel, additional noise losses can be achieved for the same amount of added weight.

6.6 Noise Optimization

The interior noise in the cabin of the aircraft shown in Fig. 1 was optimized utilizing a procedure similar to the one presented in Ref. 1. The noise transmitted by each baseline panel was estimated first. Then, the noise losses due to various combinations of add-on treatments (described in Secs. 6.3 - 6.5) were calculated. The treatment or combination of treatments which reduce the spatial average cabin noise levels to about 85 dBA for the least amount of added weight was taken as the best treatment for the sidewall. To reduce the transmitted noise levels to 85 dBA, the treatment package includes lightweight aluminum honeycomb panels, constrained layer damping tapes, acoustic blankets, thin layers of impervious septa and a limp trim panel which was isolated from the vibration of the sidewall structure. Since acoustic and thermal data of the foam materials for aircraft applications are limited, they are not included in the final add-on treatment package.

The results of the optimization study for individual panels are given in Figs. 24 - 29 and for the entire sidewall in Fig. 30. Since the amount of add-on treatments varies from one panel unit to another, the surface densities given in Fig. 30 for the sidewall are average values. The main contribution to the noise reduction shown in Figs. 24 - 30 comes from honeycomb stiffening in the low frequency range up to about 300 Hz, and acoustic absorption and limp trim panels for frequencies above 300 Hz. Honeycomb treatments are especially effective for individual panels (Nos. 4 and 6) supported by heavy frames. The function of the trim is to reduce noise as it enters directly via the airborne path through the porous acoustic blankets and to absorb the noise as it reflects off the interior surfaces. If the trim is very stiff, hard and impervious, strong double wall resonances are induced between the skin panels and the trim resulting in negative noise attenuation at that particular frequency. In addition, the cabin will reverberate with low values of noise absorption and at high interior noise levels. Unisolated,

these panels vibrate with the frames producing a loudspeaker effect. The present study indicates that soft trim panels which are isolated from the vibrations of the frames could provide positive noise attenuation in the critical frequency range of 70 - 300 Hz where the propeller noise inputs are highest. These panels can be isolated by placing foam or rubber material between the frames and the trim panel. It was found that the heaviest trim panels are in the region of the propeller plane. The surface densities of the trim panels range from about 0.1 lb/ft^2 to 1.0 lb/ft^2.

The treatment sequence for skin-stringer panels (Nos. 9, 10, 11 and 12) is similar to that for single panels (Nos. 4 and 6), but heavier honeycomb treatment and heavier trim are selected for panel Nos. 9, 10 and 11. Panel No. 12 is composed of seven unequal bays and it is partially shielded by the wing. The treatment package for this panel is relatively light as shown in Fig. 29.

The amount of treatment added on to different regions of the aircraft is given in Fig. 31. The total added weight to the aircraft is about 220 lbs. The maximum takeoff gross weight of this aircraft is 11,200 lbs. Thus, the weight of the add-on treatment is about 2% of the takeoff gross weight. A typical distribution of the surface density of the add-on treatment is presented in Fig. 32 at several locations on the sidewall. As can be observed from these results, the heaviest treatment is in the region of the propeller plane. It is assumed that in this case the propeller rotation is from below (port side). At the starboard side, it is recommended that heavier treatment be implemented for Panel Nos. 4 and 6 and the ceiling area in the vicinity of the propeller rotation plane. The final configuration of the optimized treatment is given in Fig. 31. These results show the relative contribution of different treatments for each region of the aircraft. A compar-

ison on noise transmitted through the baseline structure and that through a sidewall treated with two different add-on packages is presented in Fig. 33. The optimized treatment gives an additional 3 - 7 dBA noise reduction over the heavy package in the frequency range of 70 - 300 Hz. The basic composition of the heavy treatment is the multi-layer construction shown in Figs. 12 and 13. The weight added to the aircraft by the heavy and optimized treatments is about 290 lbs and 220 lbs, respectively.

7. Conclusions

An analytical model has been used to predict the noise transmission into a twin engine G/A aircraft under flight conditions. A relatively good agreement has been reached between theoretical predictions and experimental measurements for baseline, light and heavy treatment conditions. The average calculated noise levels of about 102 dBA in the untreated aircraft have been reduced to the optimized level of 85 dBA. The required noise reduction has been achieved mainly in the low frequency range of 70 - 300 Hz. The first three blade passage harmonics of this aircraft are in this frequency range.

The required noise reduction to achieve the selected optimization goal has been obtained by treatments which include lightweight aluminum honeycomb panels, constrained layer damping tapes, porous acoustic blankets, thin and impervious septum barriers and limp trim panels which are isolated from the vibration of the main sidewall structure. Due to the non-uniform distribution of the propeller noise pressure and the different structural dynamic characteristics of the sidewall panels, the amount and type of treatment varies from one panel unit to another. The total added weight to the aircraft is about 220 lbs which is about 2% of the total take-off gross weight. The single most effective treatment in the low frequency region is stiffening with honeycomb panels.

The theoretical predictions tend to indicate that a treatment composed of several layers of heavy septum (lead vinyl) which are separated by porous acoustic blankets does not provide proper noise attenuation in the low frequency range of 70 - 300 Hz where the propeller noise inputs are the highest. However, such a treatment is very effective for frequencies above 300 Hz. The small amount of noise attenuation in the low frequency region can be at-

tributed to the multiple double wall resonances resulting from the multi-layered treatments. Semi-rigid acoustic materials with a large value of flow resistivity could provide a significant amount of noise reduction even in the low frequency range. However, the experimental data on the acoustic properties of these materials are limited. Adding a large amount of non-load carrying mass to the aircraft skin has a positive effect on noise reduction at the second and third blade passage harmonic frequencies, but increases noise transmission at the first blade passage harmonic.

The amount of noise transmitted through the windows is relatively high for this aircraft. These estimates are based on a simple single sheet plexiglass analytical model. Most of the window units are double wall (exterior curved) plexiglass constructions. Depending on the structural dynamic characteristics of both sheets and the distance between the inner and outer units, strong double wall resonances could be induced resulting in high transmitted noise levels. To reduce these noise levels to acceptable limits, a new design for the double wall window might need to be implemented. Such a new window could include one or several of the following features: a partial vacuum between the two panes, a floating inner pane which is isolated from the vibration of the main structure, significantly different dynamic characteristics of the two panes, more than two plexiglass sheets, or a sandwich panel type construction with a transparent viscoelastic layer.

REFERENCES

1. Vaicaitis, R. and Slazak, M., "Cabin Noise Control for Twin Engine General Aviation Aircraft," NASA Contract Report 165833, February 1982.

2. Cheung, Y.K., Finite Strip Method in Structural Mechanics, Pergamon Press, 1976.

3. Chang, M.T. and Vaicaitis, R., "Noise Transmission Into Semicylindrical Enclosures Through Discretely Stiffened Curved Panels," Journal of Sound and Vibration, Vol. 85, 3, 1982.

4. Lin, Y.K. and Donaldson, B.K., "A Brief Survey of Transfer Matrix Techniques with Special References to the Analysis of Aircraft Panels," Journal of Sound and Vibration, Vol. 10, 1969, pp. 103-143.

5. Vaicaitis, R. and Slazak, M., "Noise Transmission Through Stiffened Panels," Journal of Sound and Vibration, Vol. 70, 3, 1980, pp. 413-426.

6. "A Study of Propeller Noise Research SP 67148, Hamilton Standard, United Technologies Corp., November 1967.

7. Piersol, A.G., Wilby, E.G. and Wilby, J.F., "Evaluation of AeroCommander Propeller Acoustic Data: Static Operations," NASA Contractor Report 158919, May 1978.

8. Piersol, A.G., Wilby, E.G. and Wilby, J.F., "Evaluation of AeroCommander Propeller Acoustic Data: Taxi Operations," NASA Contractor Report 159124, July 1979.

9. Beranek, L.L., "Acoustic Properties of Homogeneous, Isotropic Rigid Tiles and Flexible Blankets," Journal of the Acoustical Society of America, Vol. 19, No. 4, 1947.

10. Rennison, D.C., Wilby, J.F., Marsh, A.M. and Wilby, E.G., "Interior Noise Control Prediction Study for High-Speed, Propeller-Driven Aircraft," NASA Contractor Report 159200, September 1979. (Also AIAA-80-0998, presented at the AIAA 6th Aeroacoustics Conference, June 4-6, 1980, Hartford, Ct.).

11. Cockburn, J.A. and Jolly, A.C., "Structural Acoustic Response, Noise Transmission Losses, and Interior Noise Levels of an Aircraft Fuselage Excited by Random Pressure Fields," AFFDC-TR-68-2, August 1968, Air Force Flight Dynamics Laboratory Technical Report.

12. Dowell, E.H., Gorman, G.F., III and Smith, D.A., "Acoustoelasticity - General Theory, Acoustic Natural Modes and Forced Response to Sinusoidal Excitation, Including Comparisons with Experiments," Journal of Sound and Vibration, Vol. 52, 1977, pp. 519-592.

13. Mixson, J.S., Barton, C.K. and Vaicaitis, R., "Investigation of Interior Noise in a Twin Engine Light Aircraft," Journal of Aircraft, AIAA, Vol. 15, No. 4, April 1978, pp. 227-233.

14. Bhattacharya, M.C. and Crocker, M.J., "Forced Vibration of a Panel and Radiation of Sound Into a Room," Acustica, Vol. 22, 1969/70, pp. 273-294.

15. Vaicaitis, R., Slazak, M. and Chang, M.T., "Noise Transmission - Turboprop Problem," AIAA 5th Aeroacoustics Conference, Paper No. 79-0645, Seattle, Wa., March 1979.

16. Vaicaitis, R., "Noise Transmission Into a Light Aircraft," Journal of Aircraft, AIAA, Vol. 17, No. 2, February 1980.

17. Bleich, F., Buckling Strength of Metal Structures, McGraw-Hill, 1952.

18. Gjelsvik, A., Theory of Thin Walled Bars, John Wiley & Sons, New York, 1981.

19. Geisler, D.L., "Experimental Modal Analysis of an AeroCommander Aircraft," NASA Contractor Report 165750, September 1981.

20. Beranek, L.L., Ed., Noise and Vibration Control, McGraw-Hill, New York, 1971.

21. Bies, D.A. and Hansen, C.H., "Flow Resistance Information for Acoustical Design," Applied Acoustics, Vol. 13, 1980, pp. 357-391.

Table 1. Material and Geometric Properties of Stiffeners

Stiffener	A_S in^2	$E_S x 10^{-6}$ psi	I_X in^4	I_Y in^4	I_{XY} in^4	c_X in	c_Y in	$C \times 10^2$ in^4	C_{WS} in^6	ρ_S lb/in^3
Type 1	0.828	10.5	0.222	0.737	-0.157	-1.079	0.181	0.625	0.547	0.1
Type 2	0.579	10.5	0.111	0.368	-0.055	-0.640	0.061	0.298	0.048	0.1
Type 3	0.370	10.5	0.037	0.244	0.012	-0.857	0.278	0.143	0.025	0.1

Table 2. Input Noise Levels

Blade Passage Harmonics H_z	Panel Unit Number Sound Pressure Levels, dB 1	2&3	4	5	6	7&8	9	10	11	12
75	132	134	134	134	130	130	131	134	128	128
150	130	128	125	130	127	125	130	126	127	125
225	124	127	123	127	125	120	120	125	126	120
300	119	124	122	124	121	118	119	124	124	118
375	117	123	121	122	118	116	117	123	122	116
450	116	121	120	120	117	115	116	121	121	115
525	114	120	118	118	115	111	114	120	119	114
600	112	118	116	116	113	110	112	118	117	112
675	110	116	114	114	111	109	110	116	115	110
750	108	114	112	112	104	108	108	114	113	108
825	106	110	108	108	107	106	108	110	110	106
900	104	108	107	107	106	106	107	108	108	106
975	104	105	106	105	106	105	106	106	106	105
1050	104	103	106	104	106	104	105	105	106	105
Base	99	103	106	106	104	101	100	103	106	100

Table 3. Material and Geometric Properties of Panels

Panel Unit Number	$Ex10^{-6}$ psi	t_1 in	$\bar{\rho}$ lb/in^3	L_X in	L_Y in	a_o in	b_o in	ν
1	0.56	0.25	0.044	15.00	14.40	7.50	29.00	0.3
2	0.56	0.25	0.044	13.75	13.15	37.00	29.00	0.3
3	0.56	0.25	0.044	13.75	13.13	60.00	29.00	0.3
4	10.5	0.063	0.100	9.00	18.00	78.00	27.00	0.3
5	0.56	0.25	0.044	13.75	13.13	88.00	29.00	0.3
6	10.5	0.063	0.100	11.54	18.00	104.00	27.00	0.3
7	0.56	0.25	0.044	13.75	11.80	117.00	29.00	0.3
8	0.56	0.25	0.044	13.75	11.00	140.00	24.00	0.3
9	10.5	0.063	0.100	32.00	26.50	0.00	0.00	0.3
10	10.5	0.063	0.100	27.00	26.50	32.00	0.00	0.3
11	10.5	0.063	0.100	45.00	26.50	59.00	0.00	0.3
12	10.5	0.063	0.100	65.00	26.50	104.00	0.00	0.3

Table 4. Natural Frequencies of Sidewall Panels (Baseline)

Panel Unit	Frequencies Hz						
1	114,	222,	246,	352,	400,	534,	665
2&3	171,	352,	363,	540,	659,	843,	1092
4	167,	245,	360,	420,	488,	509,	693
5	182,	362,	402,	579,	664,	748,	927
6	126,	204,	265,	315,	440,	456,	492
7&8	201,	380,	468,	646,	687,	845,	1074
9	143,	157,	179,	196,	232,	237,	278
10	166,	170,	196,	212,	217,	254,	278
11	134,	171,	231,	225,	271,	292,	293
12	139,	188,	241,	262,	320,	337,	348

Table 5. Natural Frequencies for Panels Stiffened with Honeycomb (t_2 = 0.016 in)

Panel Unit	Frequencies Hz						
4	547,	803,	1177,	-	-	-	-
6	449,	730,	948,	1122,	1192,	-	-
9	211,	250,	260,	314,	341,	485,	565
10	232,	270,	286,	345,	430,	533,	622
11	198,	235,	244,	245,	368,	456,	531
12	205,	244,	252,	305,	374,	470,	548

Table 6. Natural Frequencies of Stiffened Sidewall Panels Treated with Damping Tape

Number of Spans	Frequencies, Hz			
	Added Surface Density, lb/ft^2			
	0	0.25	0.5	1.0
2	123, 156	111, 140	101, 128	89, 111
	239, 298	230, 284	220, 264	205, 248
	312, 350	302, 340	246, 330	283, 317
3	117, 138, 159	106, 122, 142	96, 113, 126	85, 47, 112
	236, 265, 301	222, 252, 285	215, 240, 270	202, 219, 248
	311, 343, 350	301, 331, 340	242, 321, 331	283, 304, 318
4	136, 148, 172, 191	123, 134, 155, 173	112, 122, 141, 161	100, 108. 124, 138
	250, 280, 247, 314	241, 270, 286, 248	233, 261, 275, 284	220, 243, 257, 262
	317, 363, 377, 400	309, 352, 363, 384	301, 342, 353, 372	292, 327, 334, 355

Table 7. Natural Frequencies of Sidewall Panels Treated with Mass Addition

Panel Unit Number	Frequencies, Hz								
	Untreated			Treated					
	0 lb/ft^2			1 lb/ft^2			2 lb/ft^2		
4	167,	245,	360	116,	169,	248	94,	138,	202
6	126,	204,	265	87,	141,	183	70,	114,	149
9	143,	157,	179	103,	113,	183	79,	87,	99
10	166,	170,	196	120,	122,	141	91,	94,	108
11	134,	171,	231	96,	123,	166	74,	94,	124
12	139,	188,	241	100,	136,	174	76,	104,	133

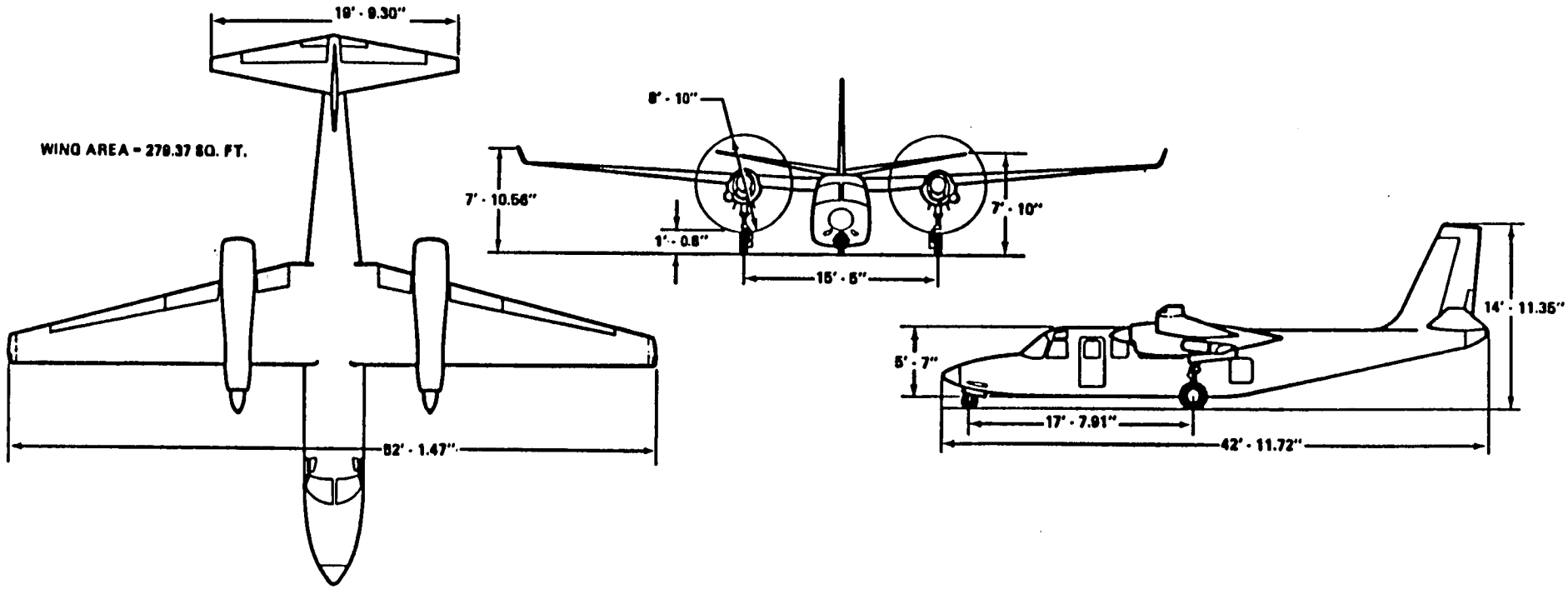

Fig. 1 Twin-engine aircraft used in noise transmission study

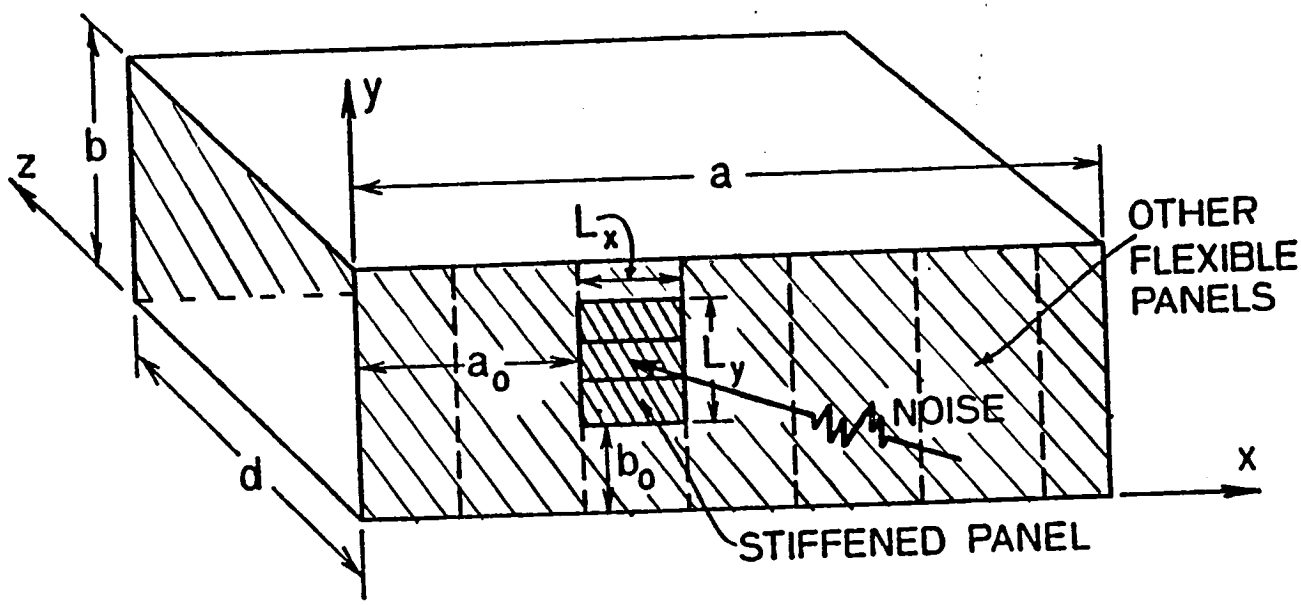

Fig. 2 Simplified geometry of aircraft cabin

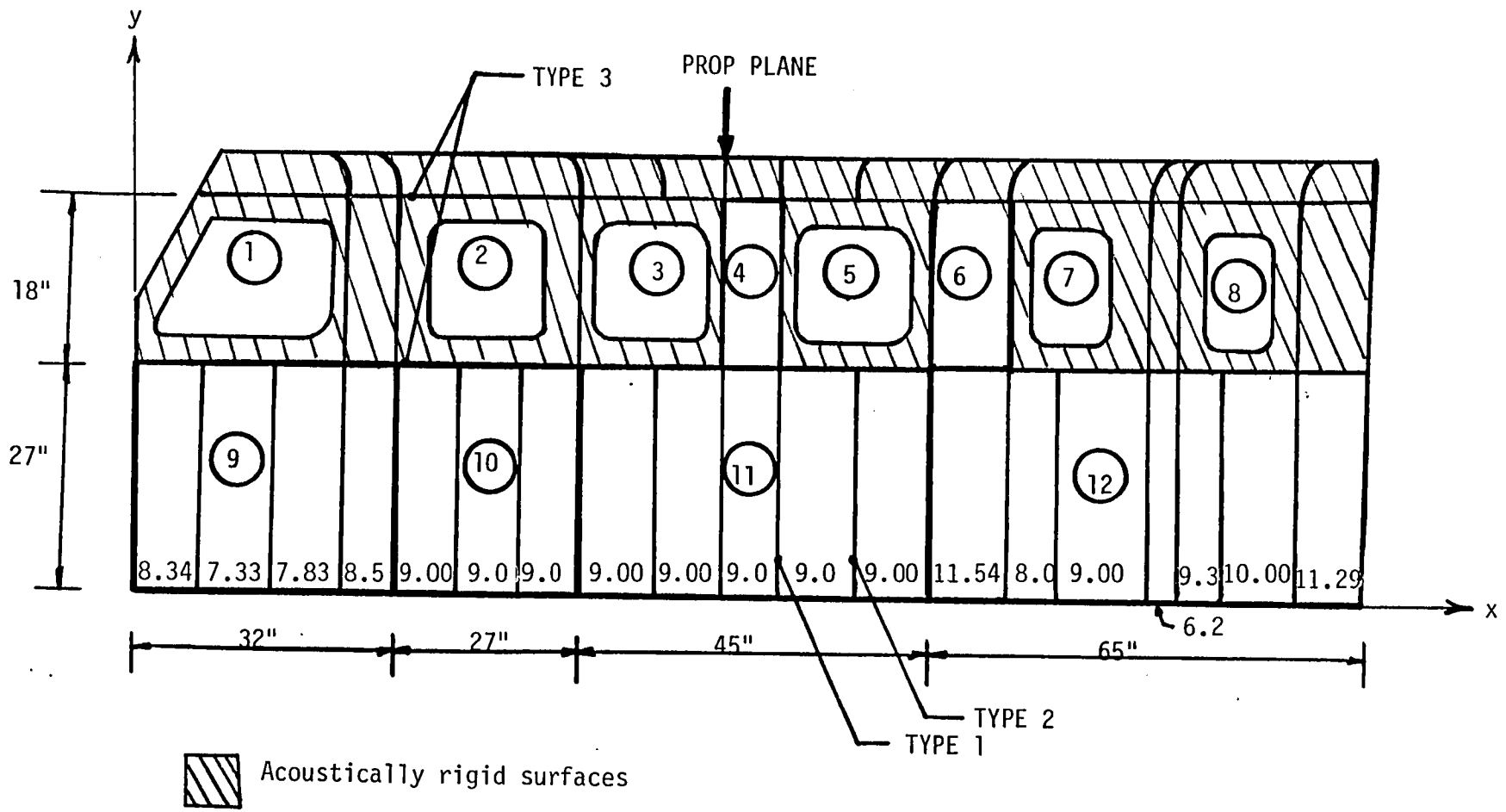

Fig. 3 Aircraft sidewall used for noise transmission study

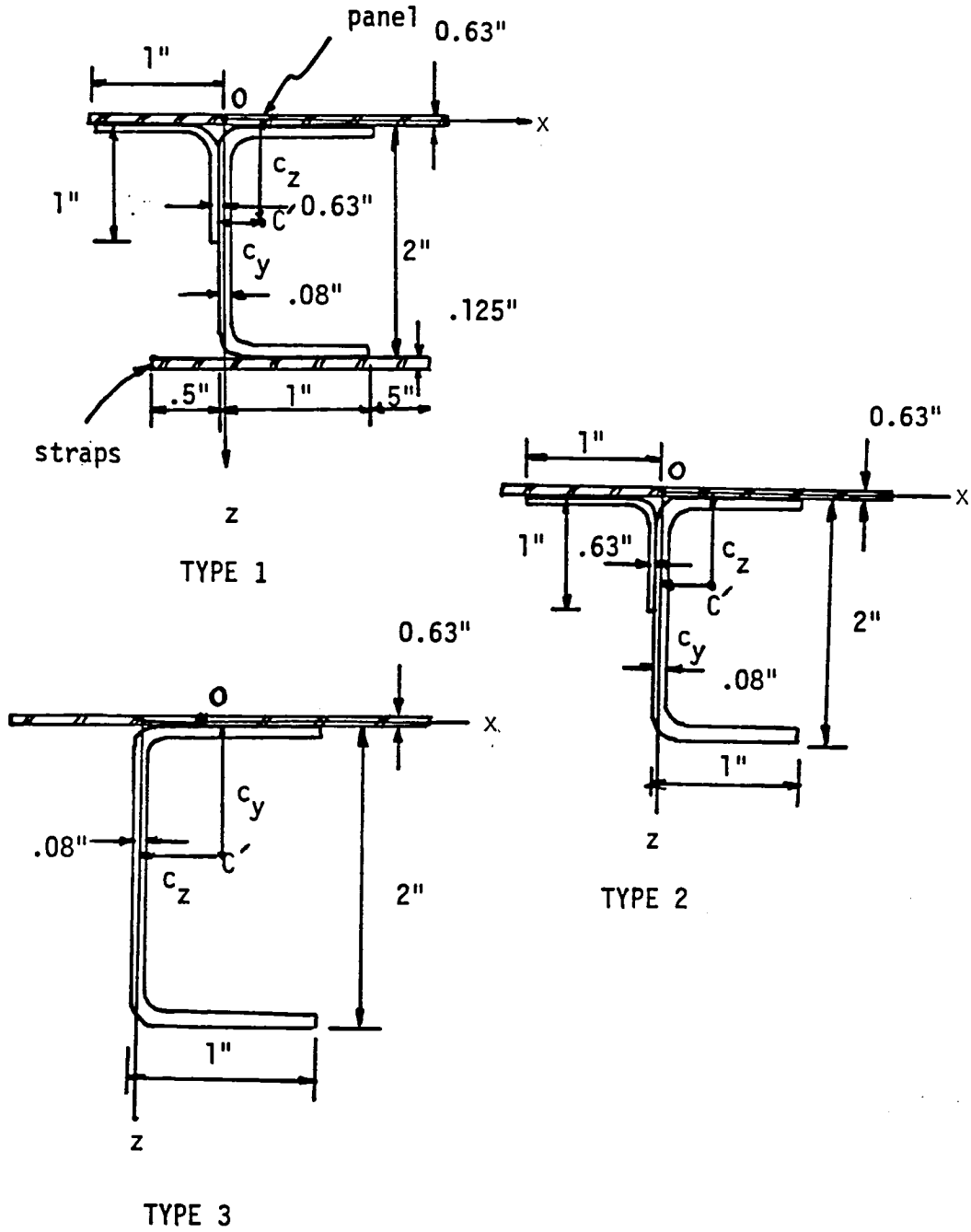

Fig. 4 Details of frame construction

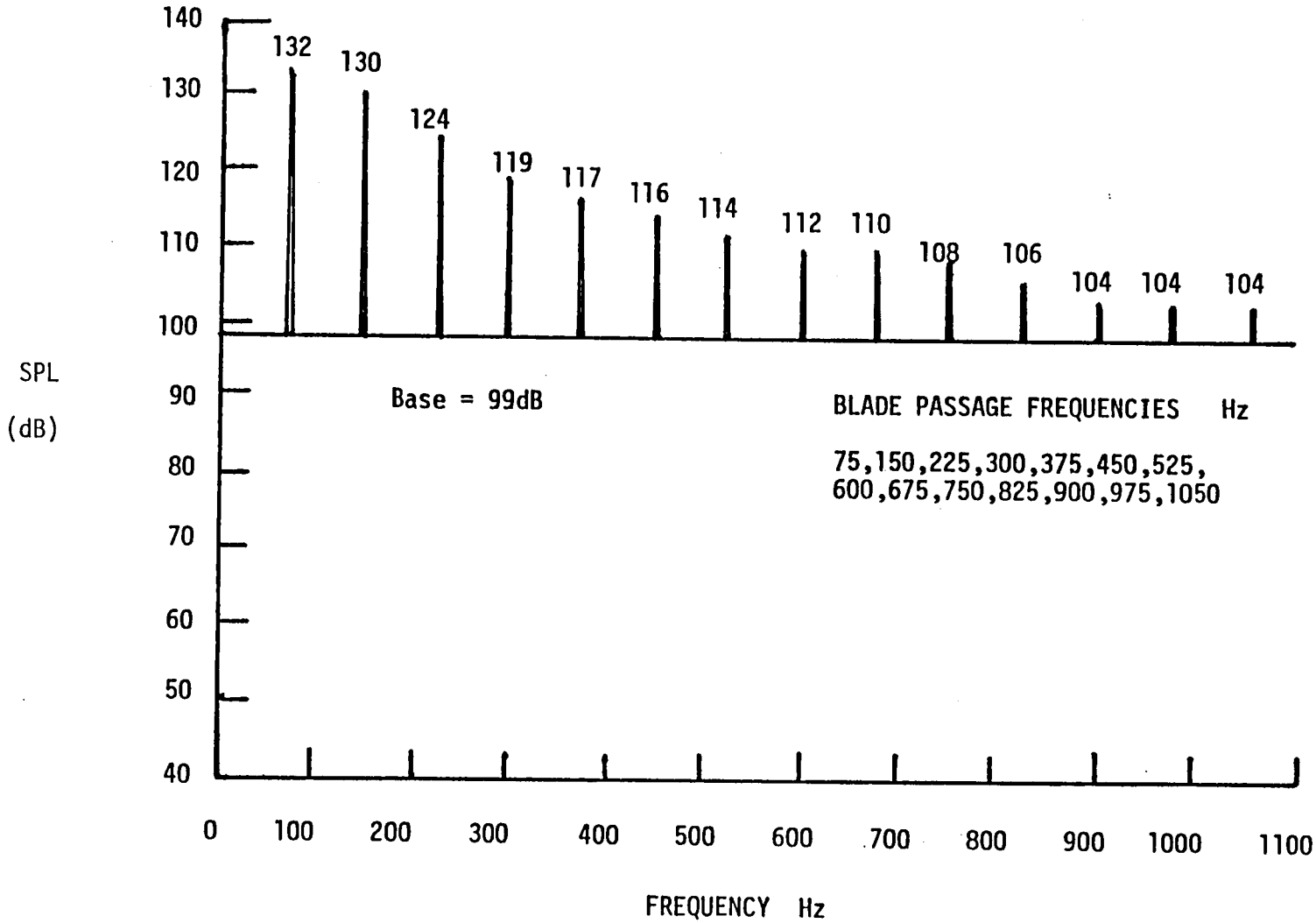

Fig. 5 Propeller noise input (panel unit no. 1)

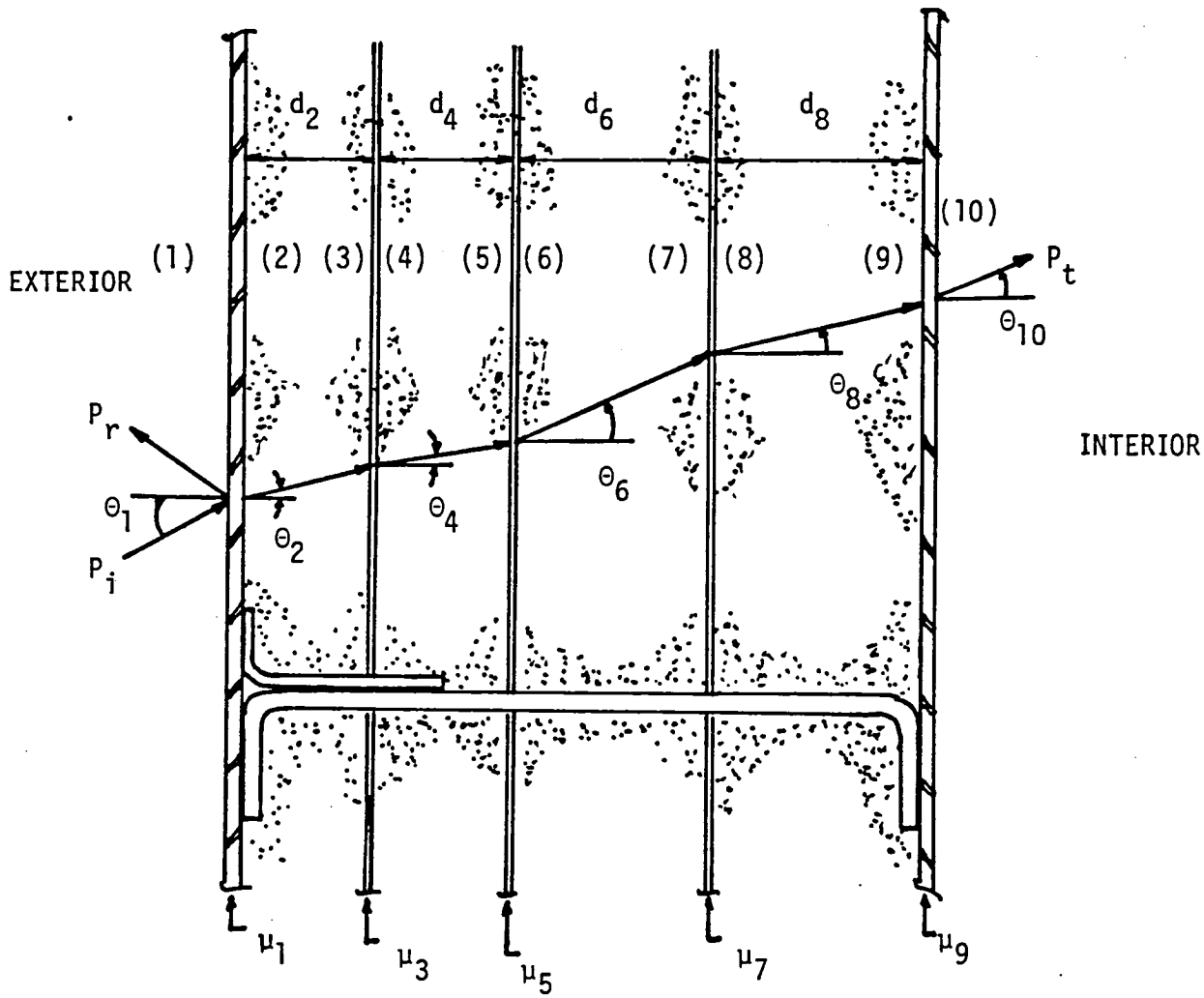

Fig. 6 Geometry of add-on sidewall treatment

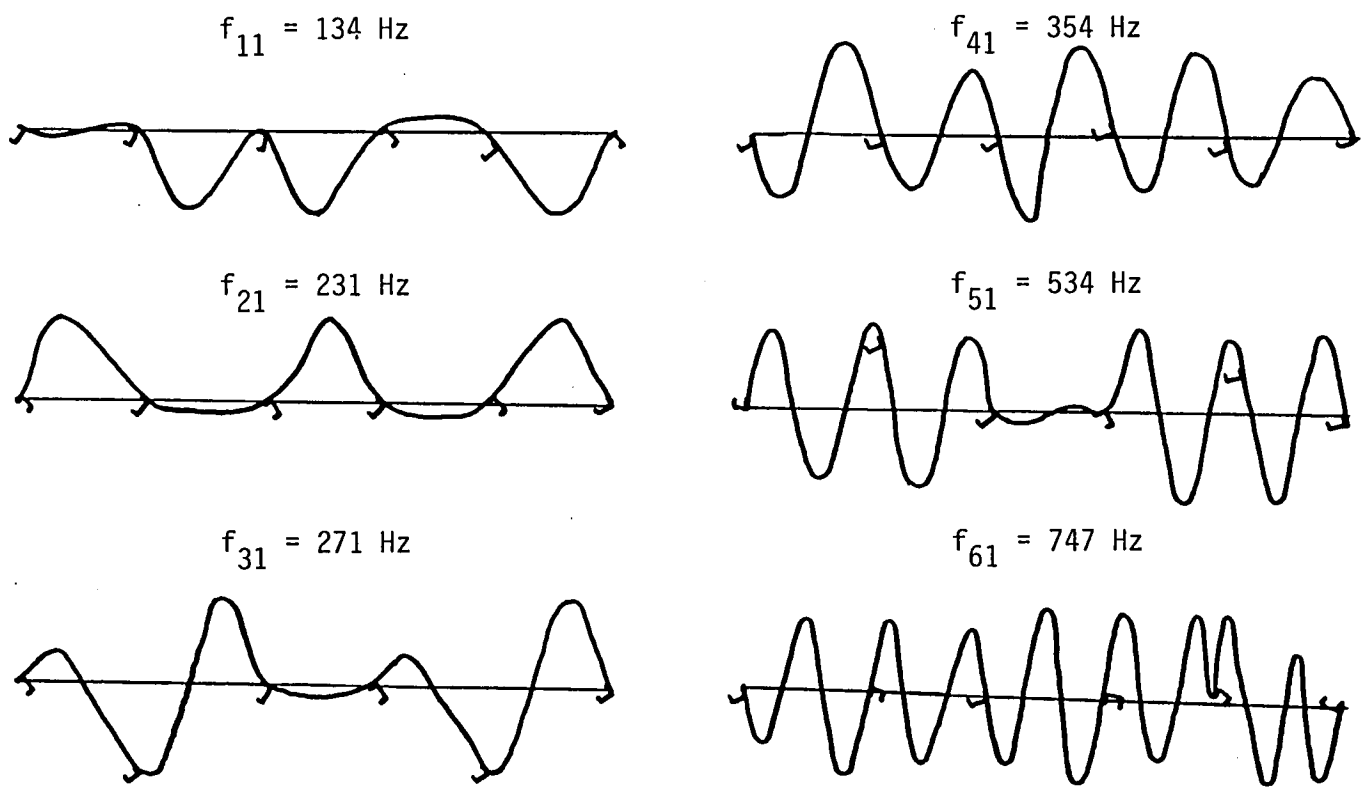

Fig. 7 Mode shapes of a skin-stringer panel (panel unit no. 11)
(n = 1, modes 1-6, baseline)

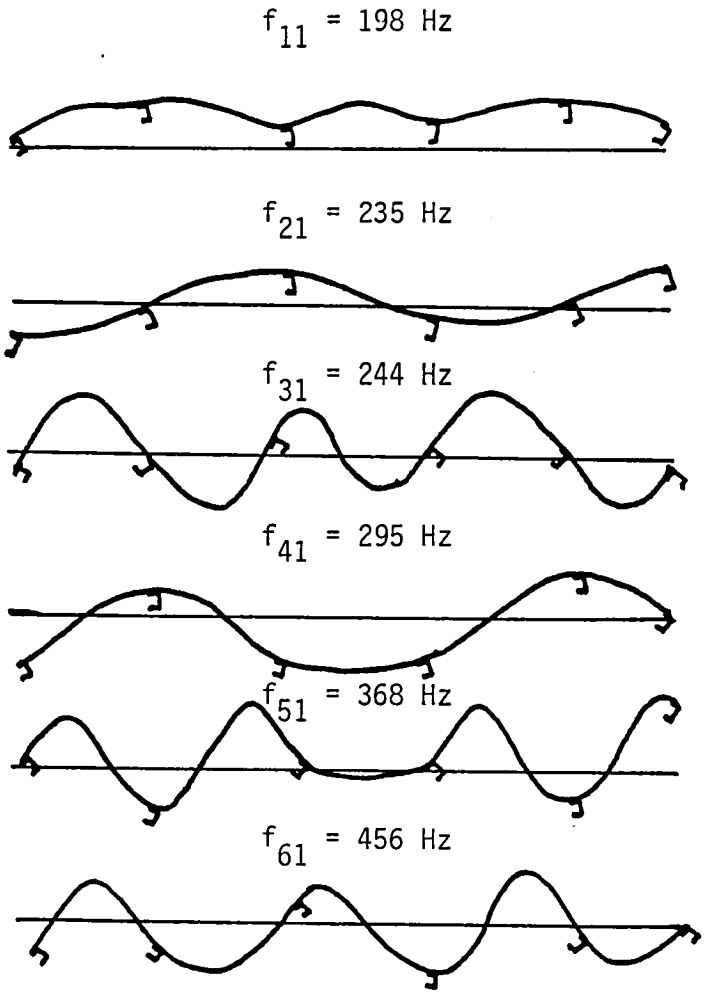

Fig. 8 Mode shapes of a skin-stringer panel stiffened with honeycomb panels (n = 1, modes 1-6, panel no. 11)

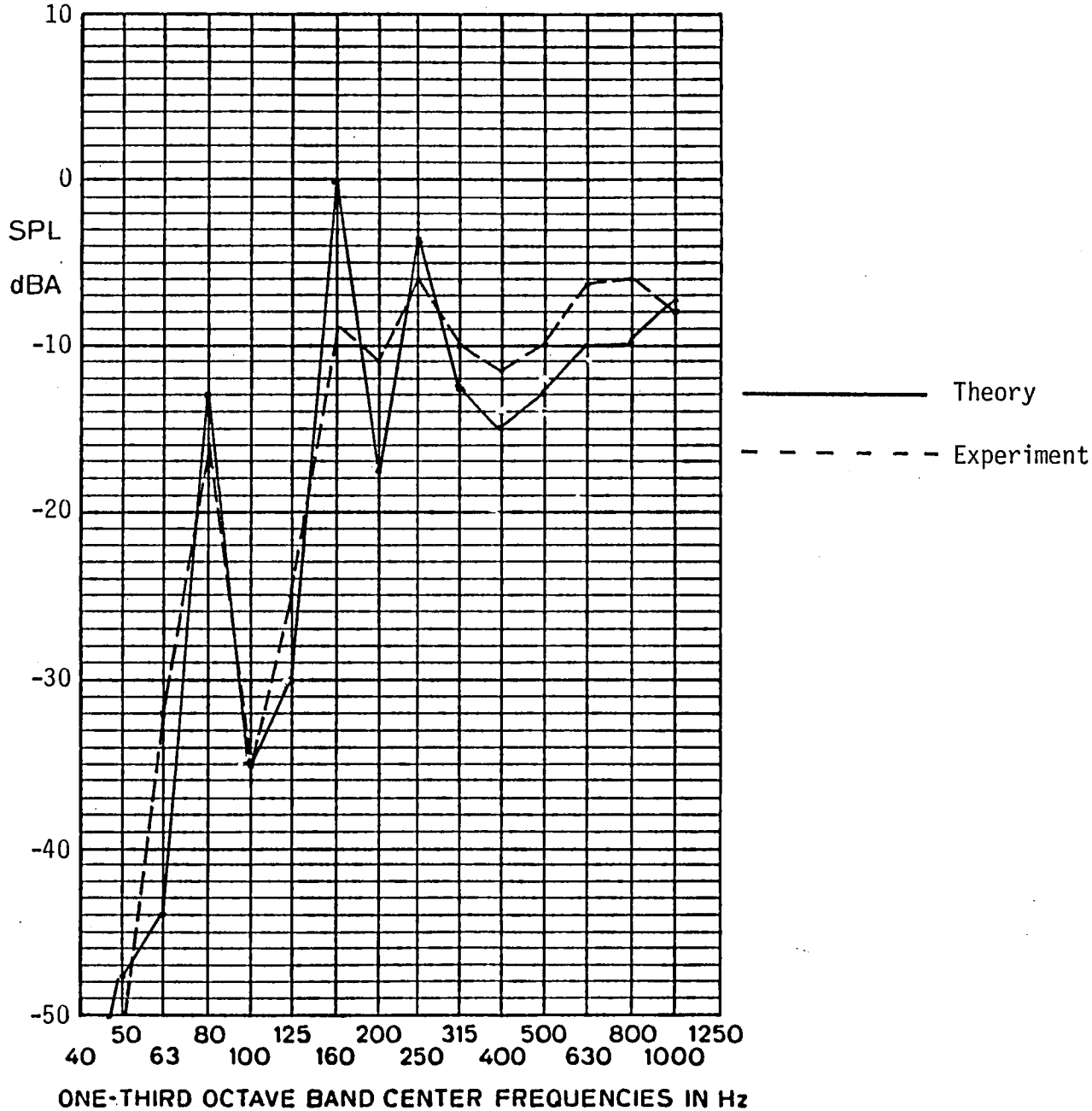

Fig. 9 Interior noise levels (baseline aircraft)

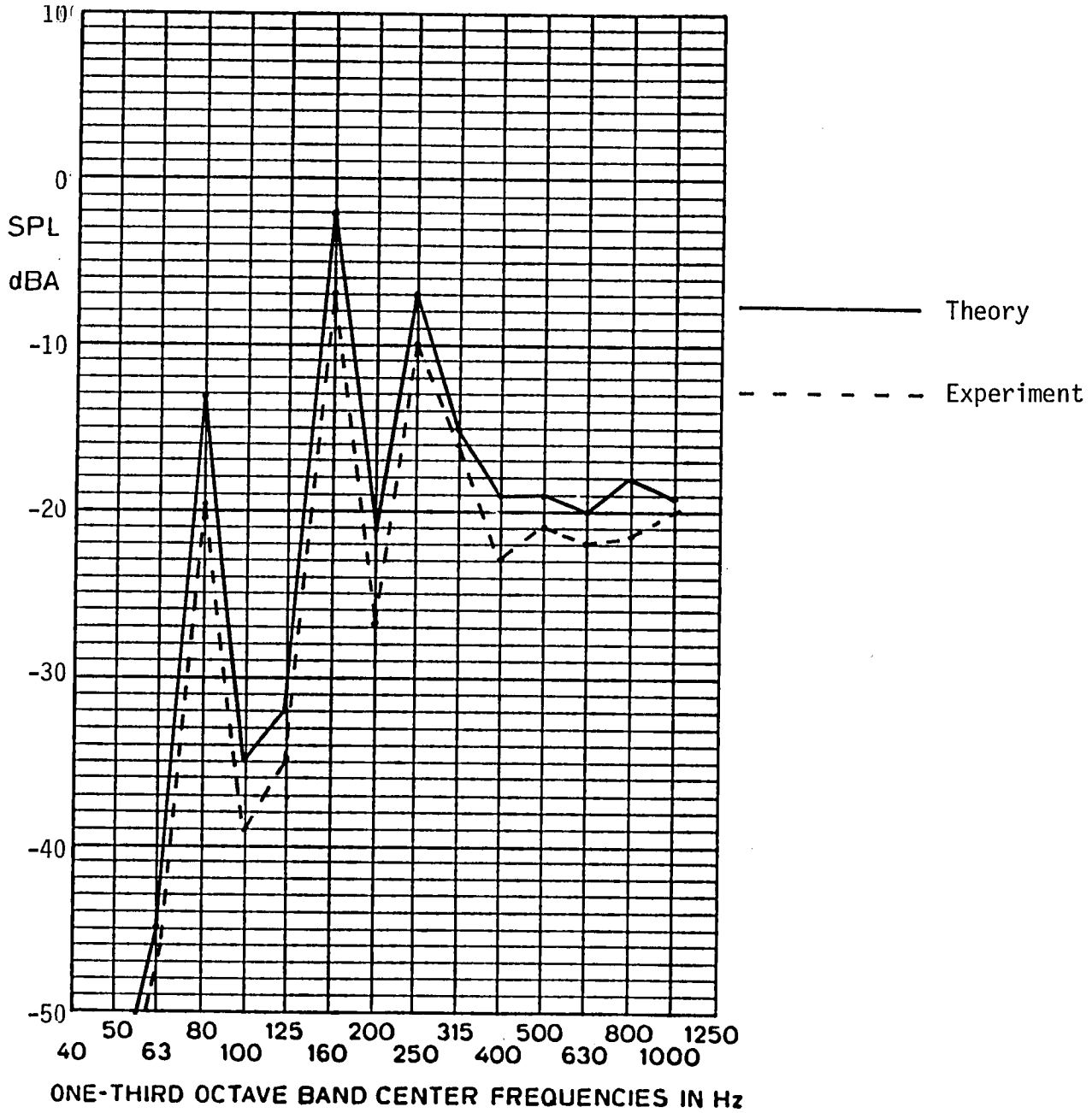

Fig. 10 Interior noise levels for aircraft treated with 2" fiberglass blankets

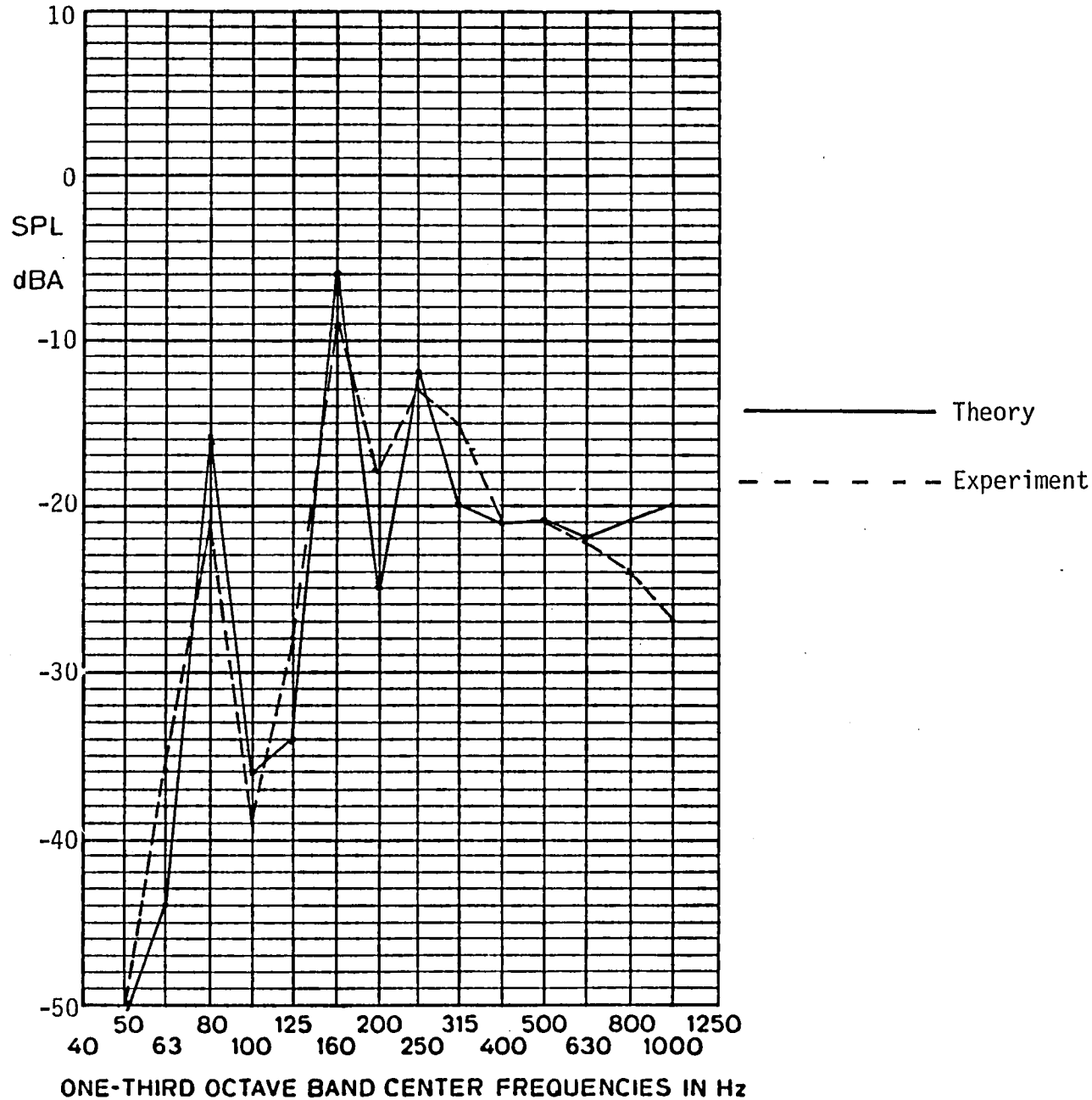

Fig. 11 Interior noise levels for aircraft treated with a heavy add-on package

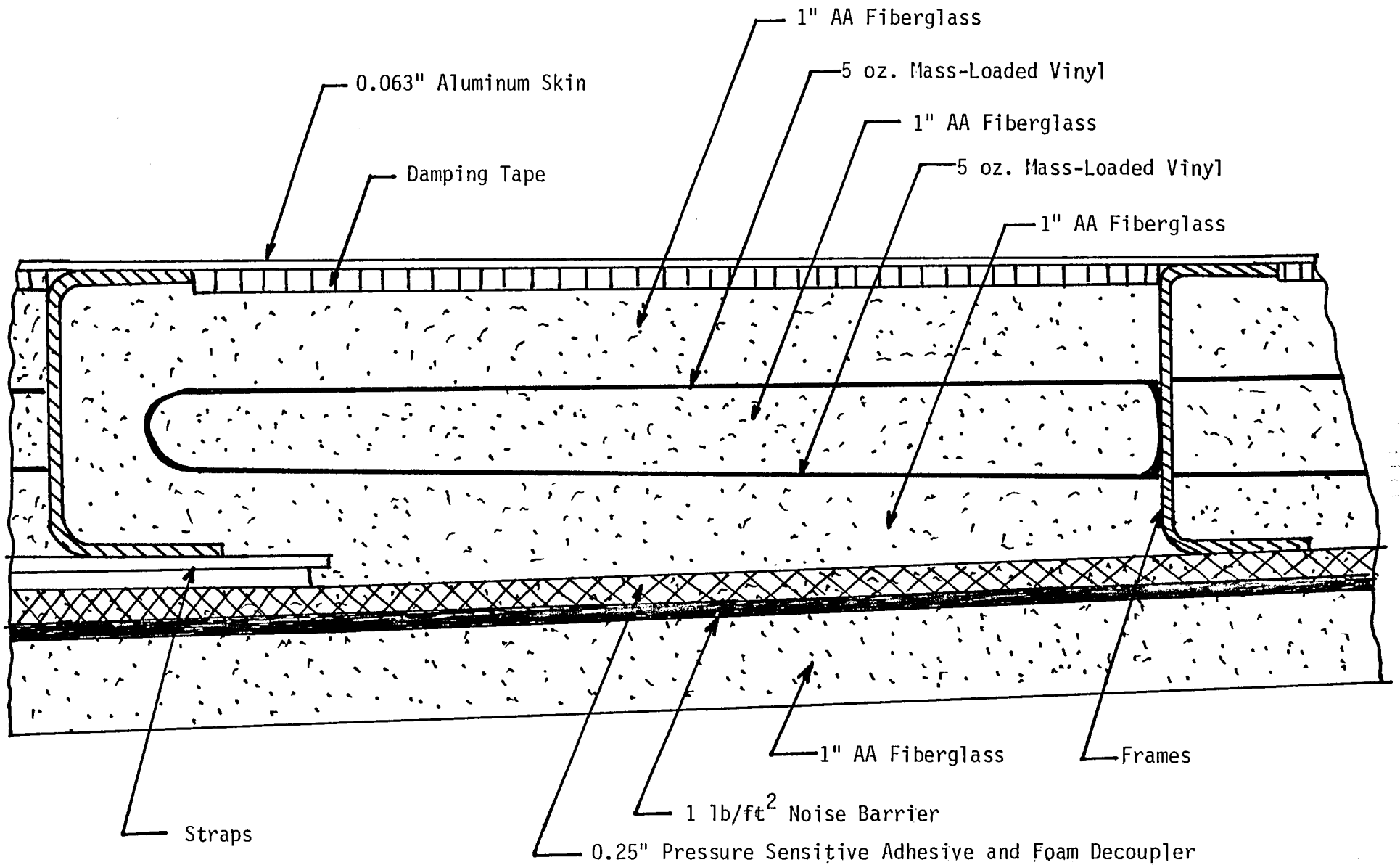

Fig. 12 Typical section in the area of the propeller rotation plane of a heavy add-on treatment

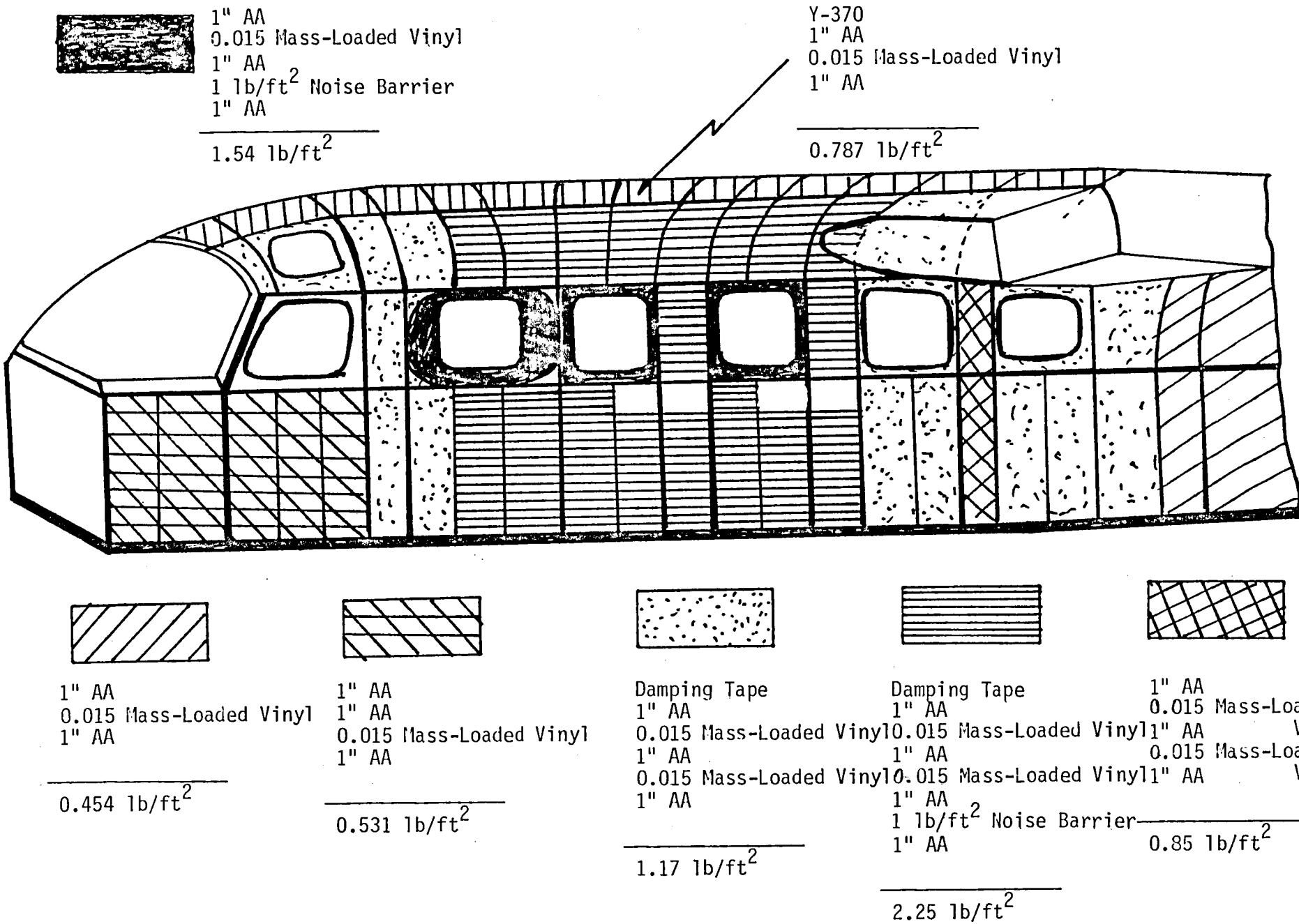

Fig. 13 Distribution of a heavy add-on treatment

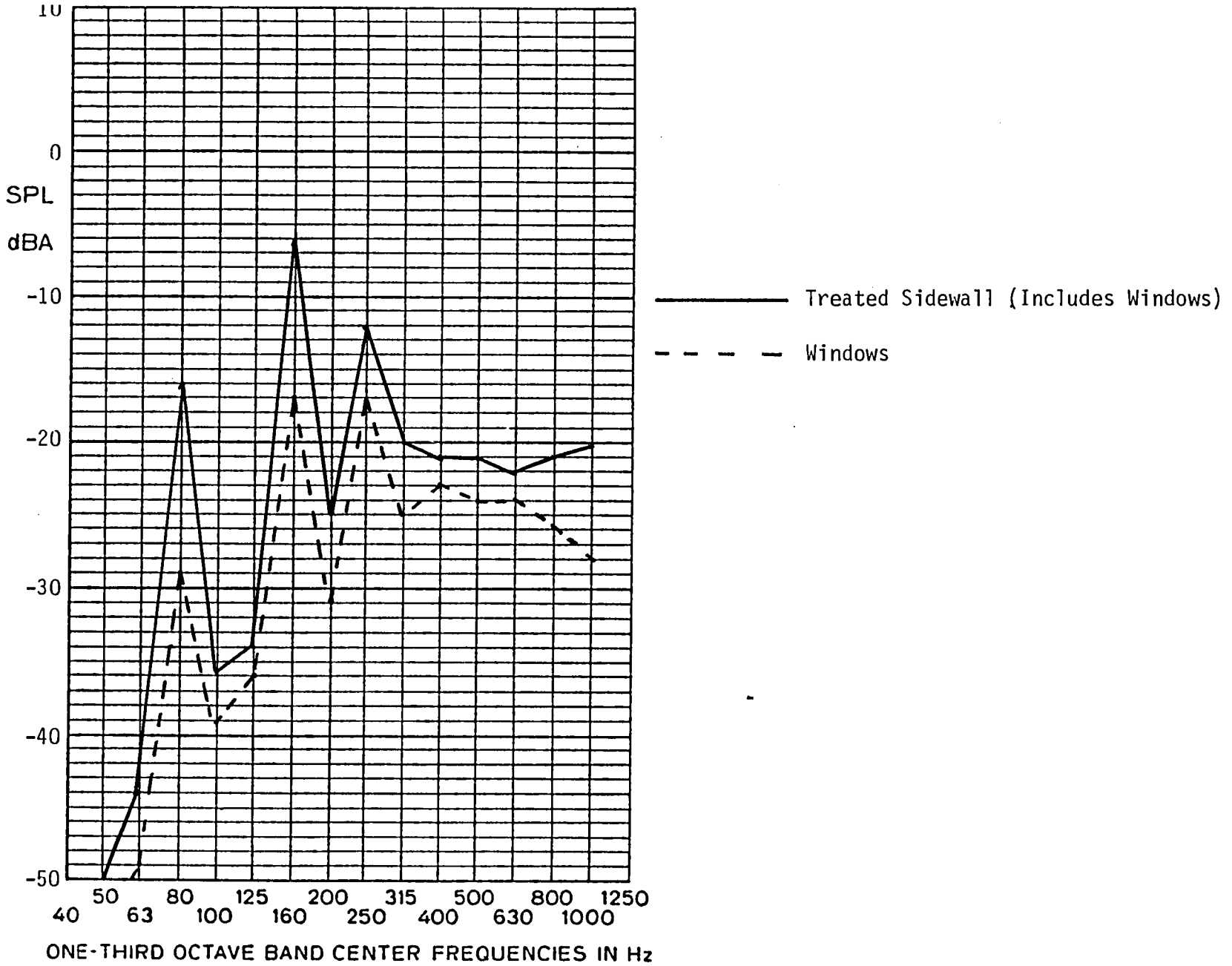

Fig. 14 Transmitted noise through windows and treated sidewall

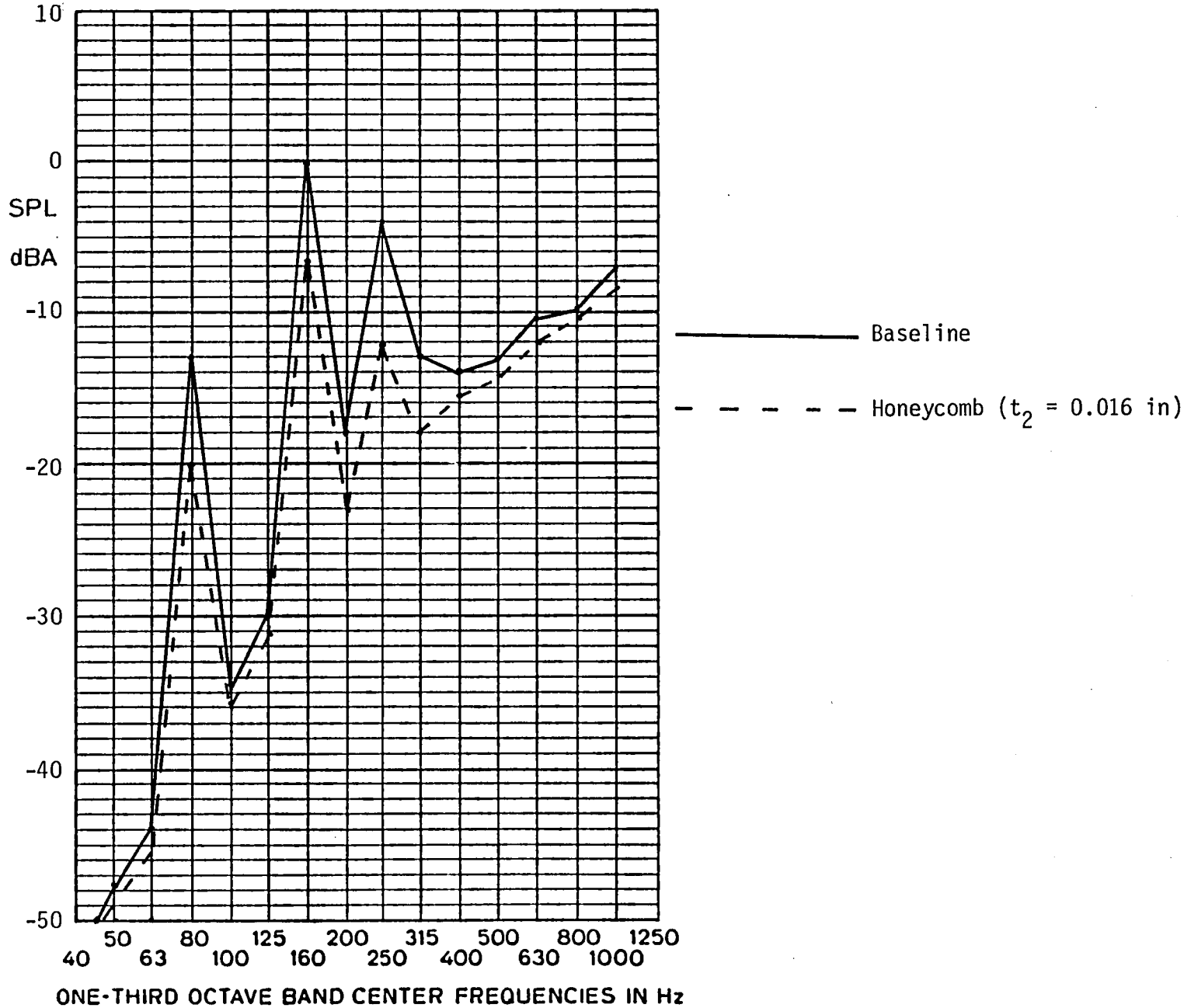
10
0
SPL
dBA
-10
-20
-30
-40
-50
40
50
63
80
100
125
160
200
250
315
400
500
630
800
1000
1250
ONE-THIRD OCTAVE BAND CENTER FREQUENCIES IN Hz
Baseline
Honeycomb (t_2 = 0.016 in)

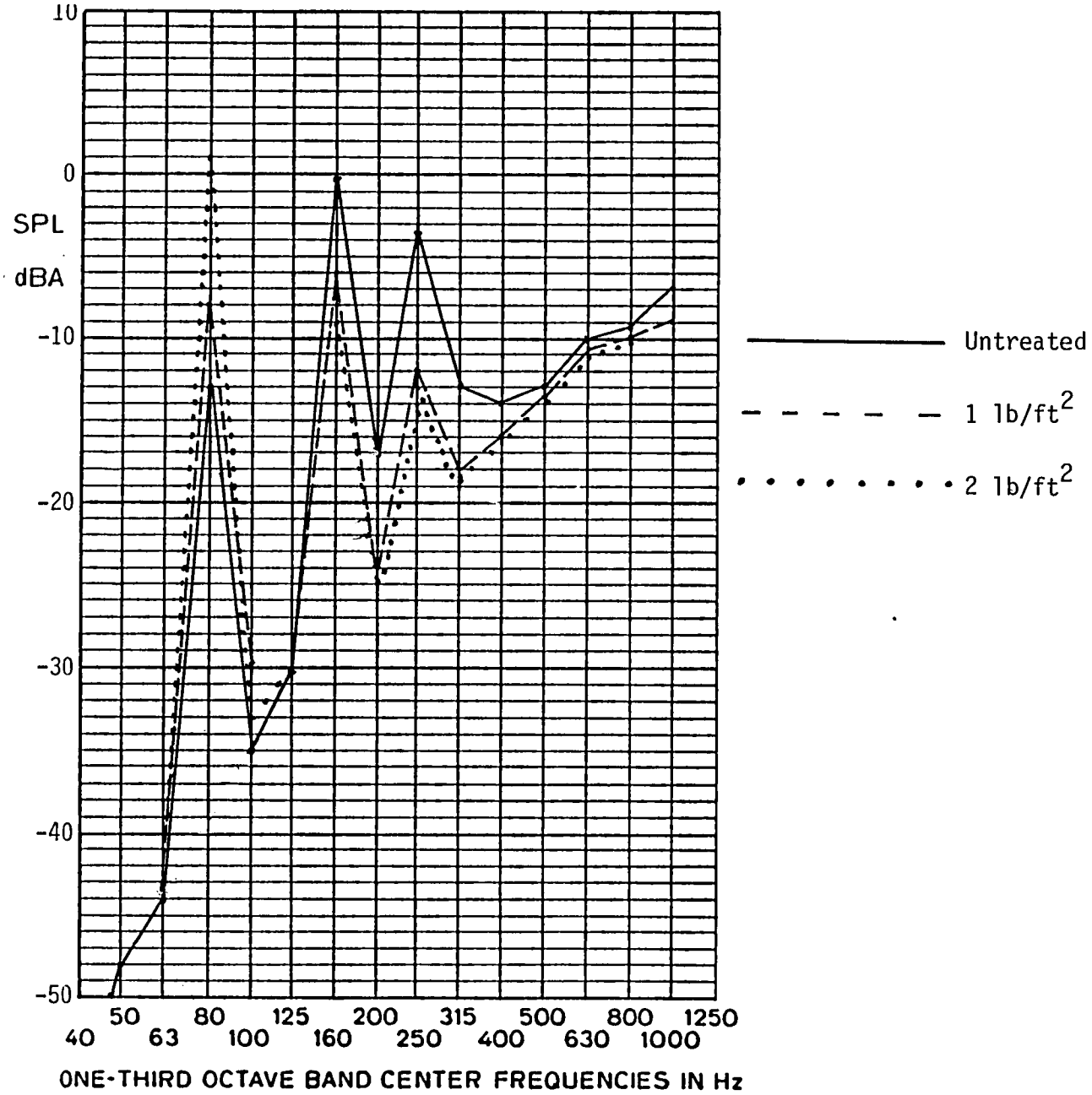

Fig. 16 Interior noise levels for damping tape and mass add-on treatments

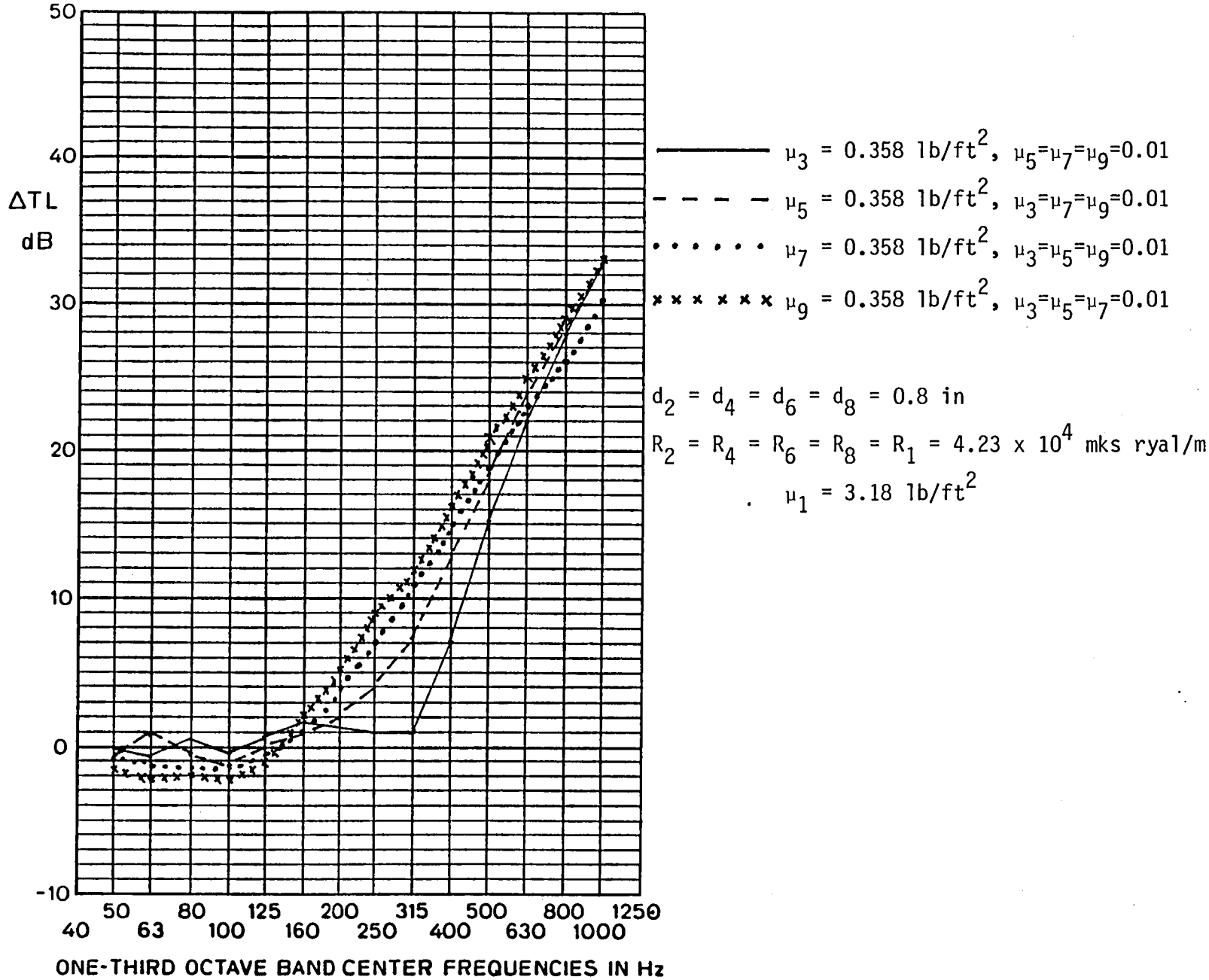

Fig. 17 Additional noise losses for different locations of septum barrier (medium weight septum)

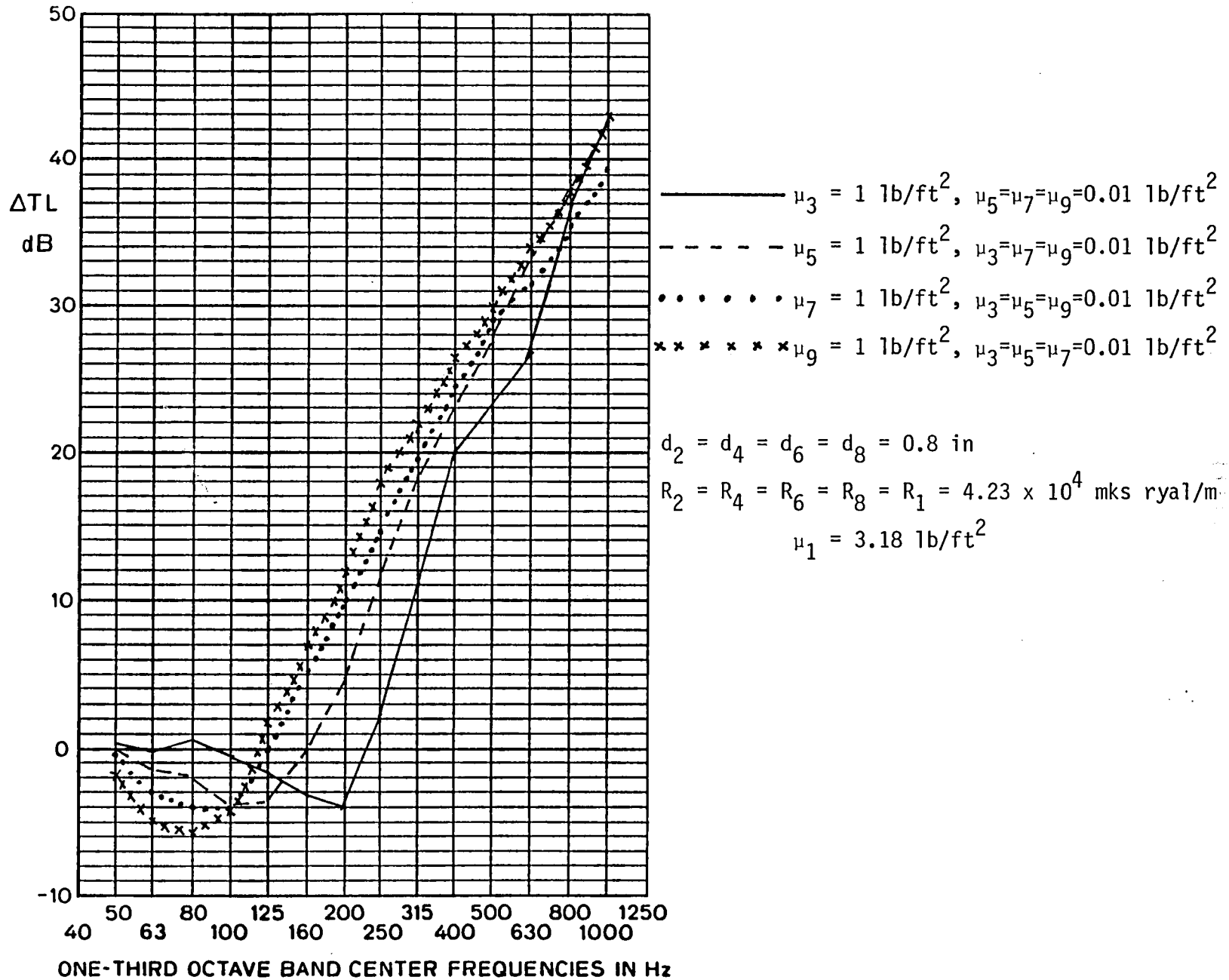

Fig. 18 Additional noise losses for different locations of septum barrier (heavy weight treatment)

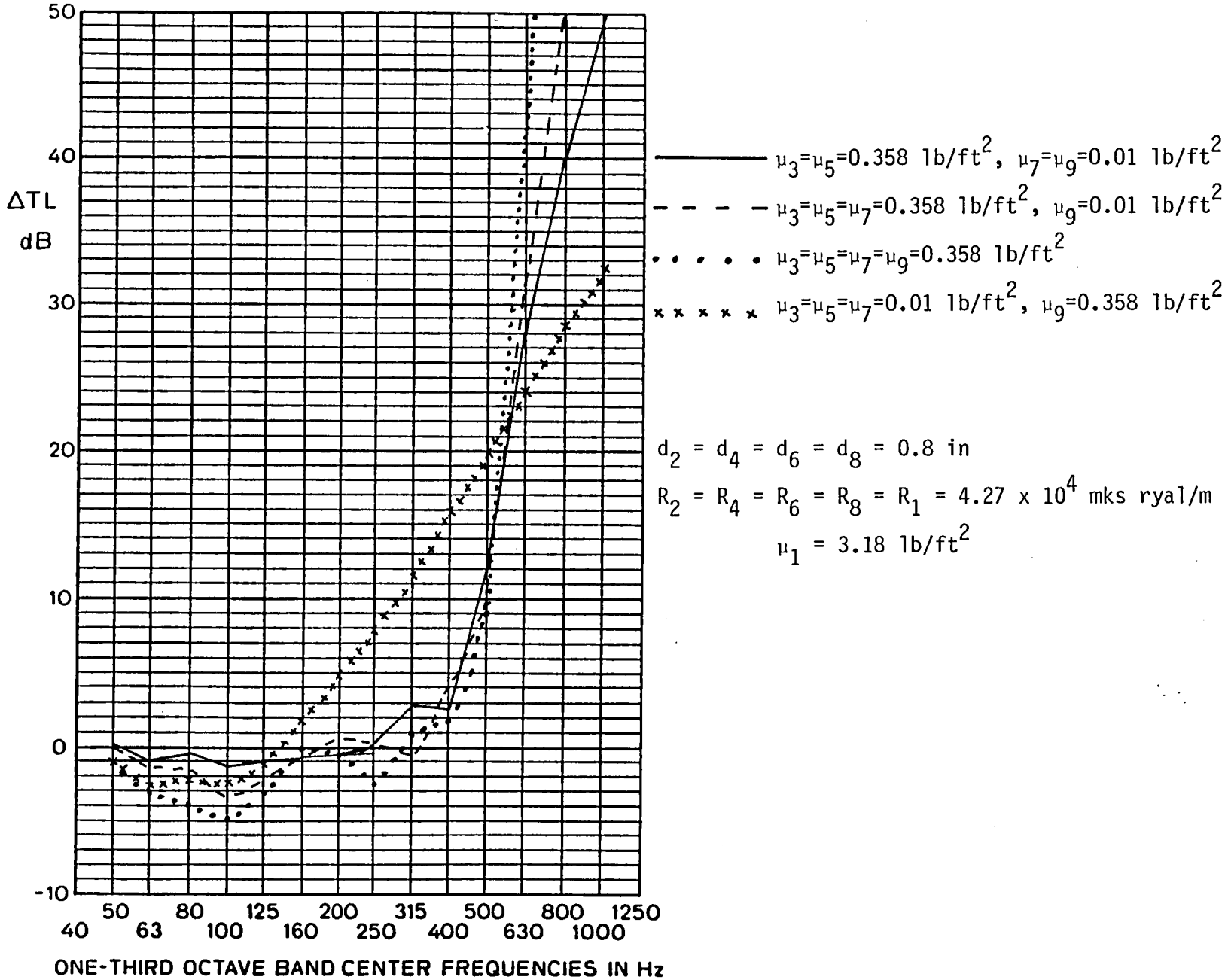

Fig. 10 Additional noise losses for different surface densities of acoustic septum barriers

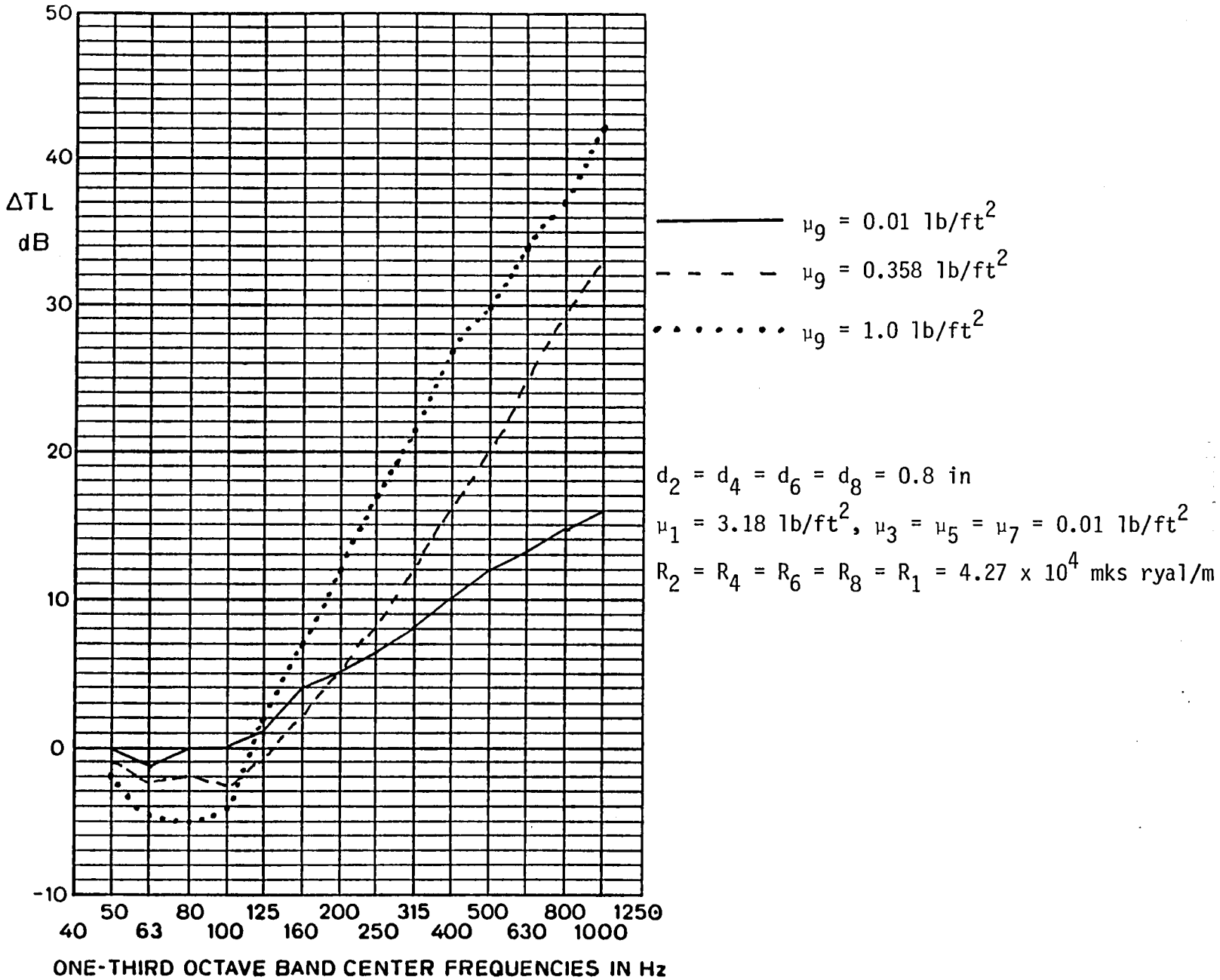

Fig. 20 Additional noise losses for different surface densities of trim panel

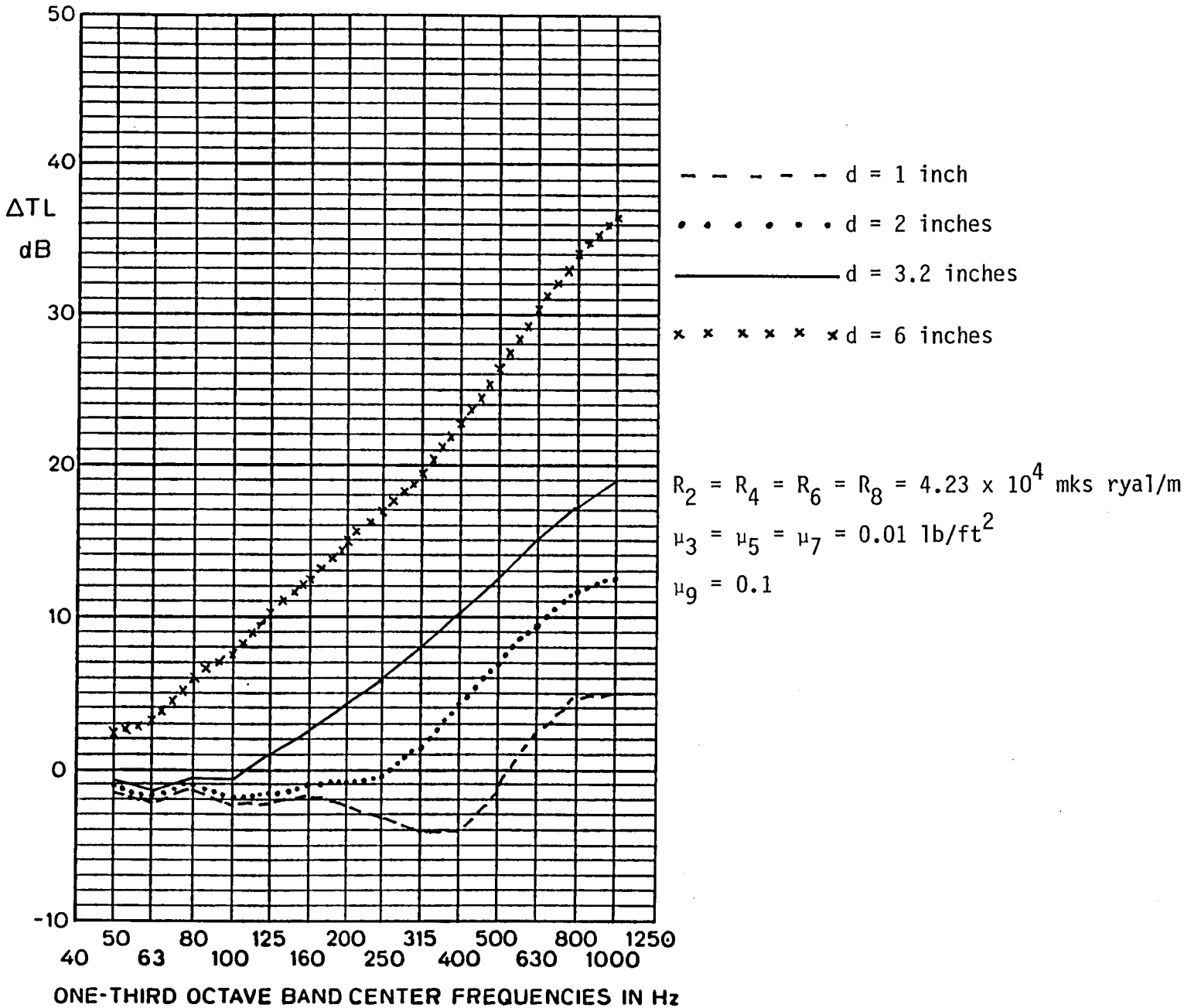

Fig. 21 Additional noise losses for different cavity depths

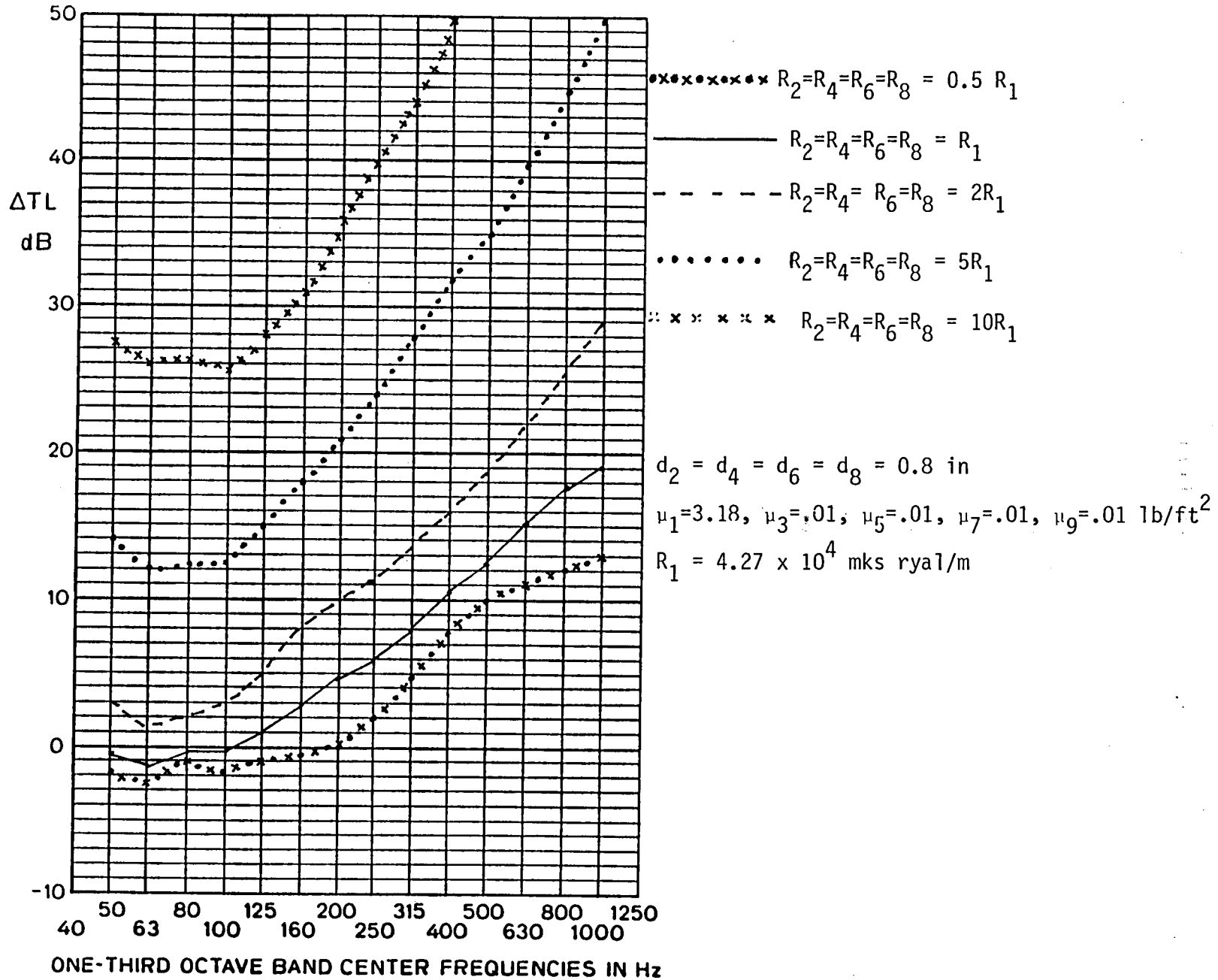

Fig. 22 Additional noise losses for a treatment composed of acoustic blankets and semi-rigid materials

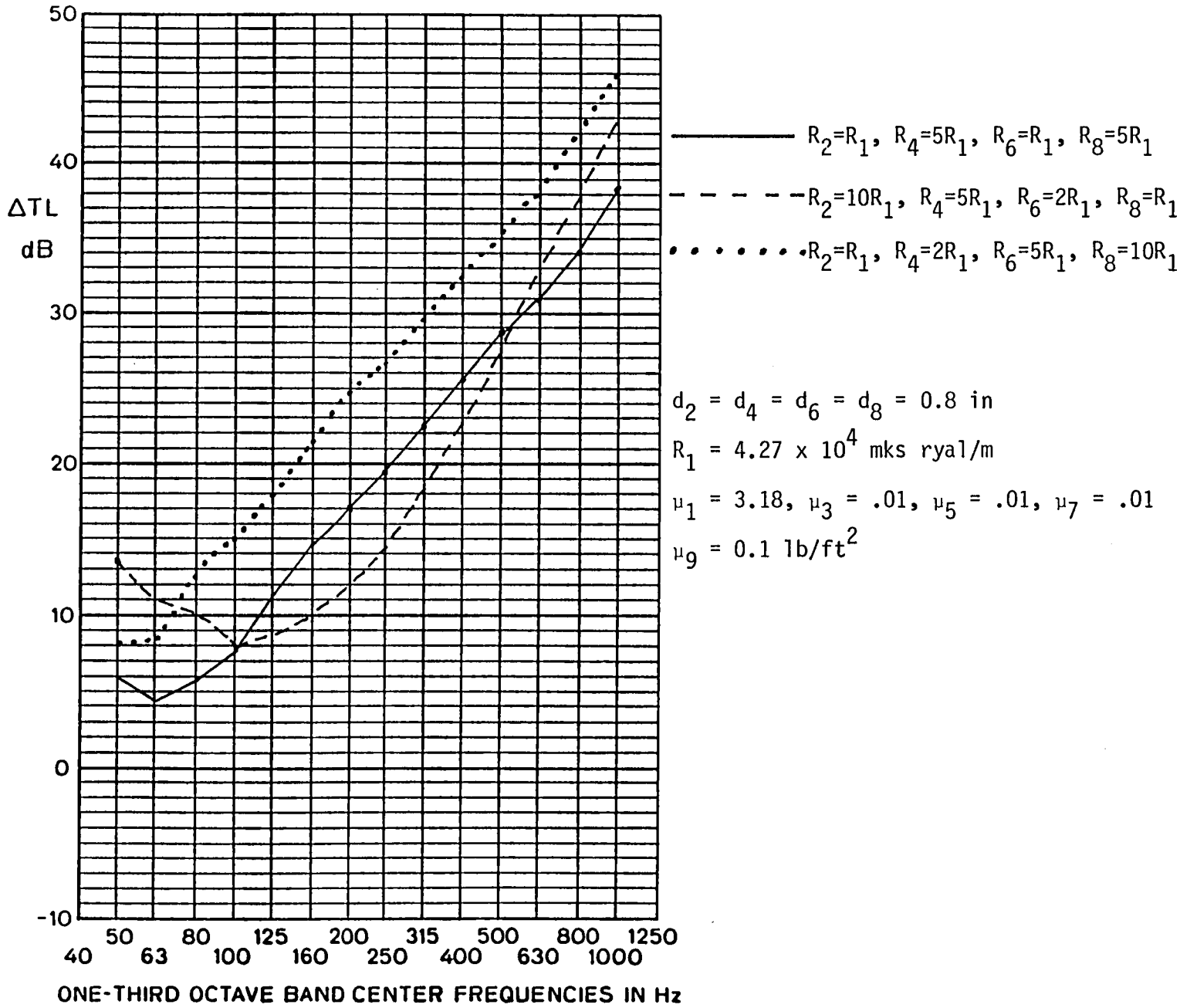

Fig. 23 Additional noise losses for a treatment composed of semi-rigid materials with different resistivity coefficients

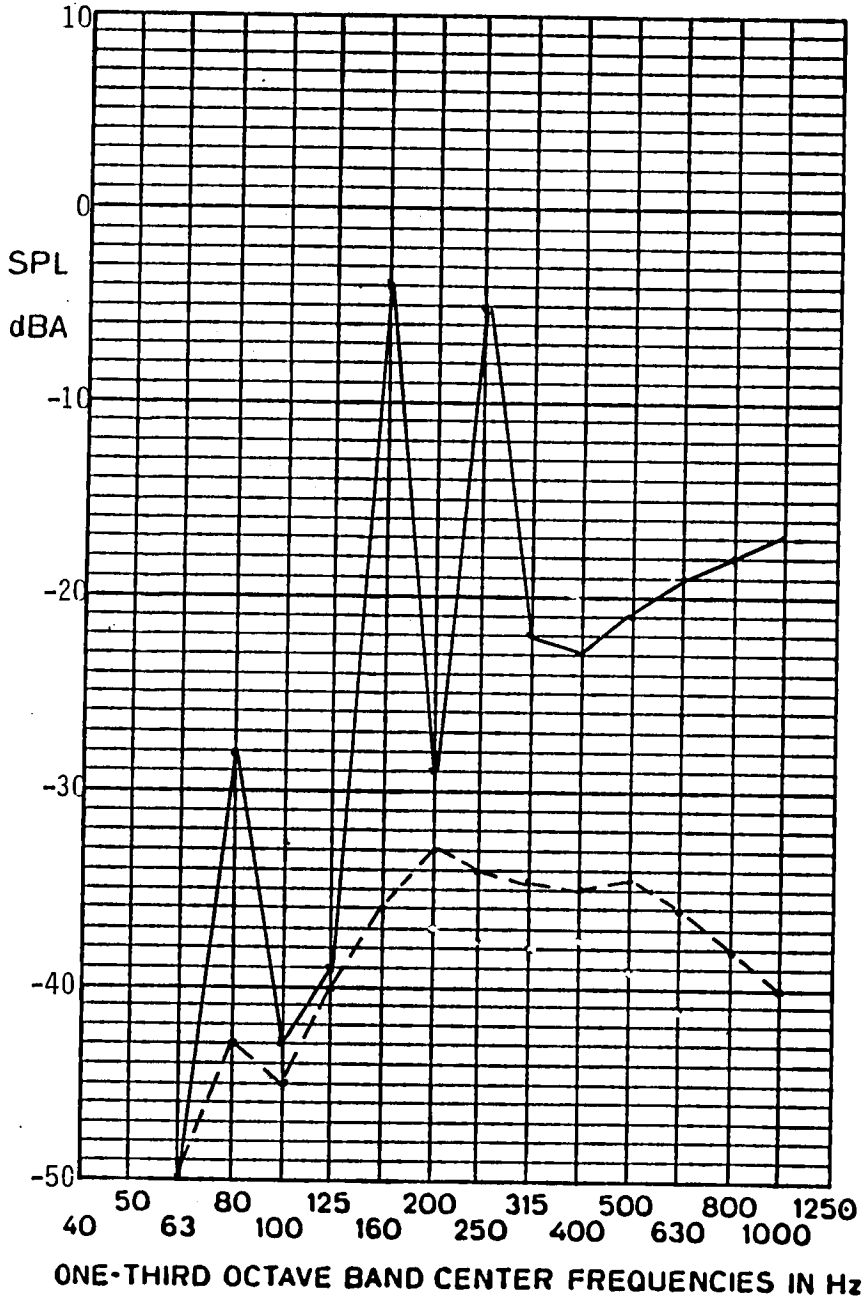

Panel Area = 1.25 ft^2

Add-on Surface Density = 1.15 lb/ft^2

Added Weight = 1.3 lbs

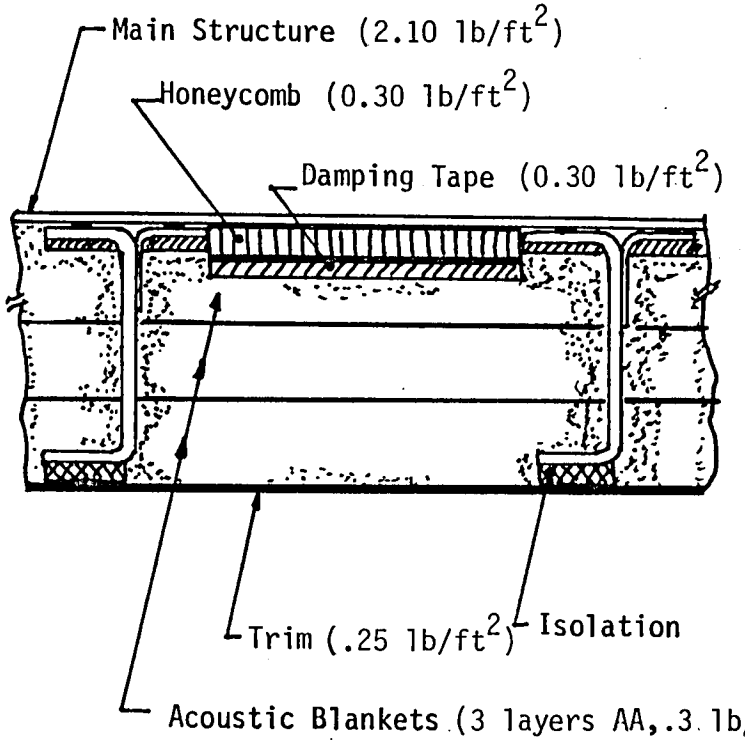

untreated

treated

Fig. 24 Transmitted noise for treated and untreated panel (No. 4)

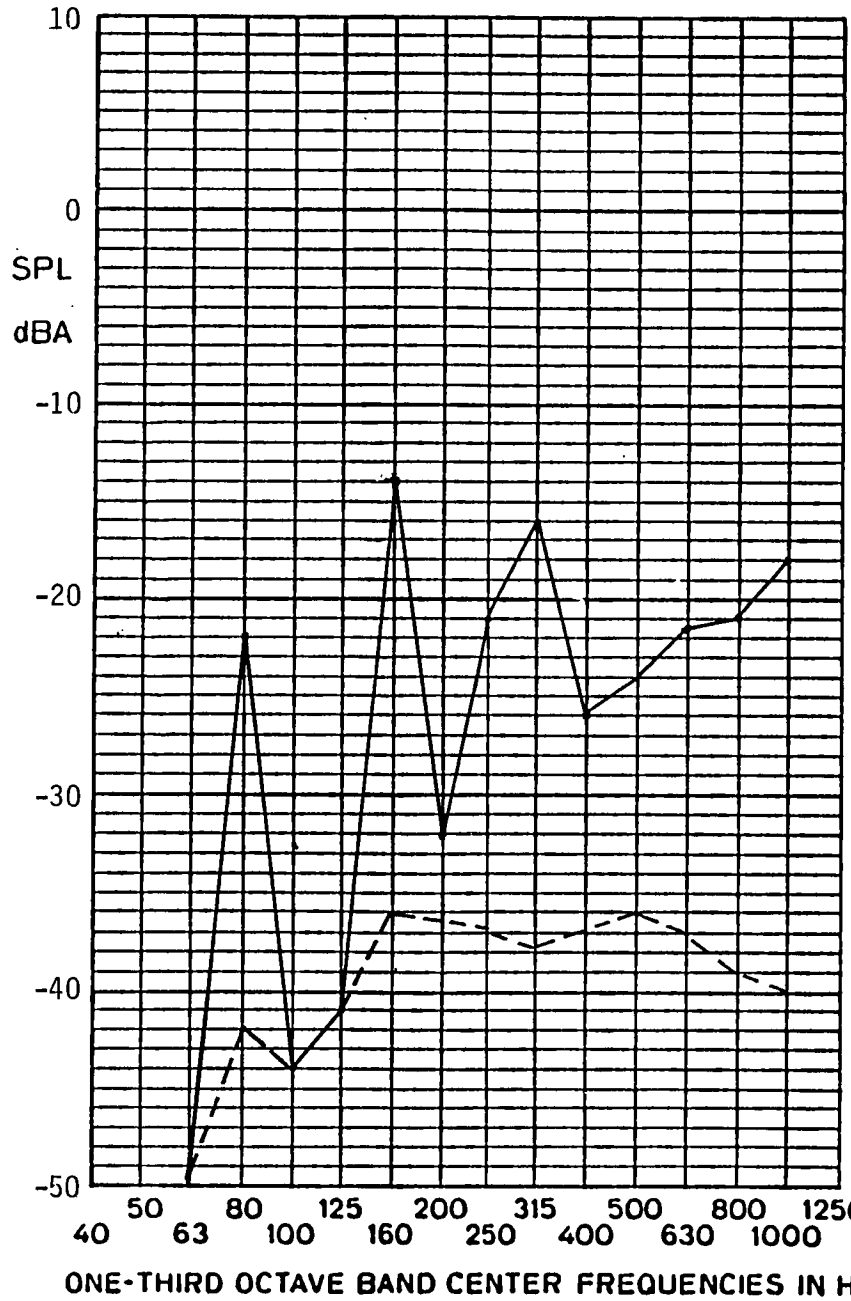

Panel Area = 1.44 ft^2

Add-on Surface Density = 1.15 lb/ft^2

Added Weight = 1.66 lbs

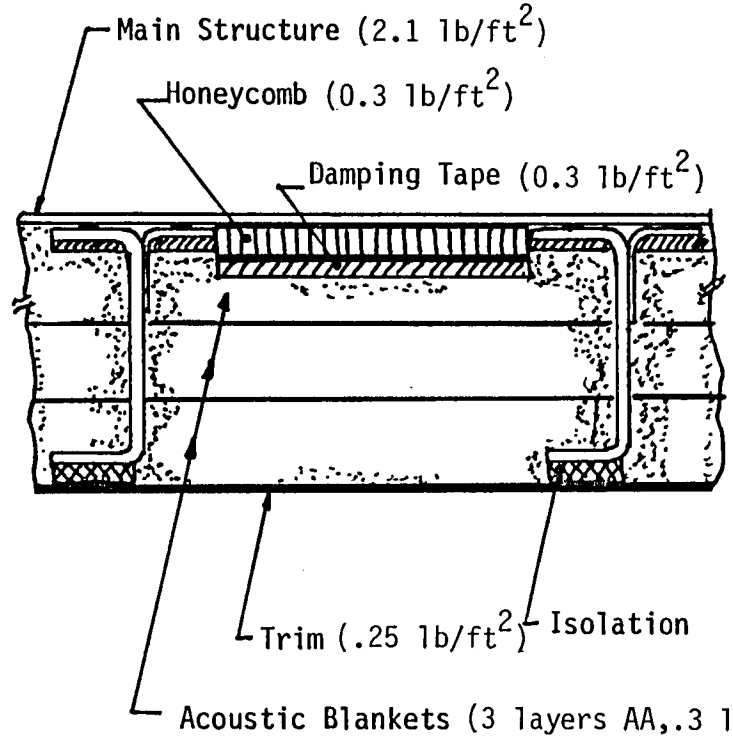

——— untreated

– – – – – treated

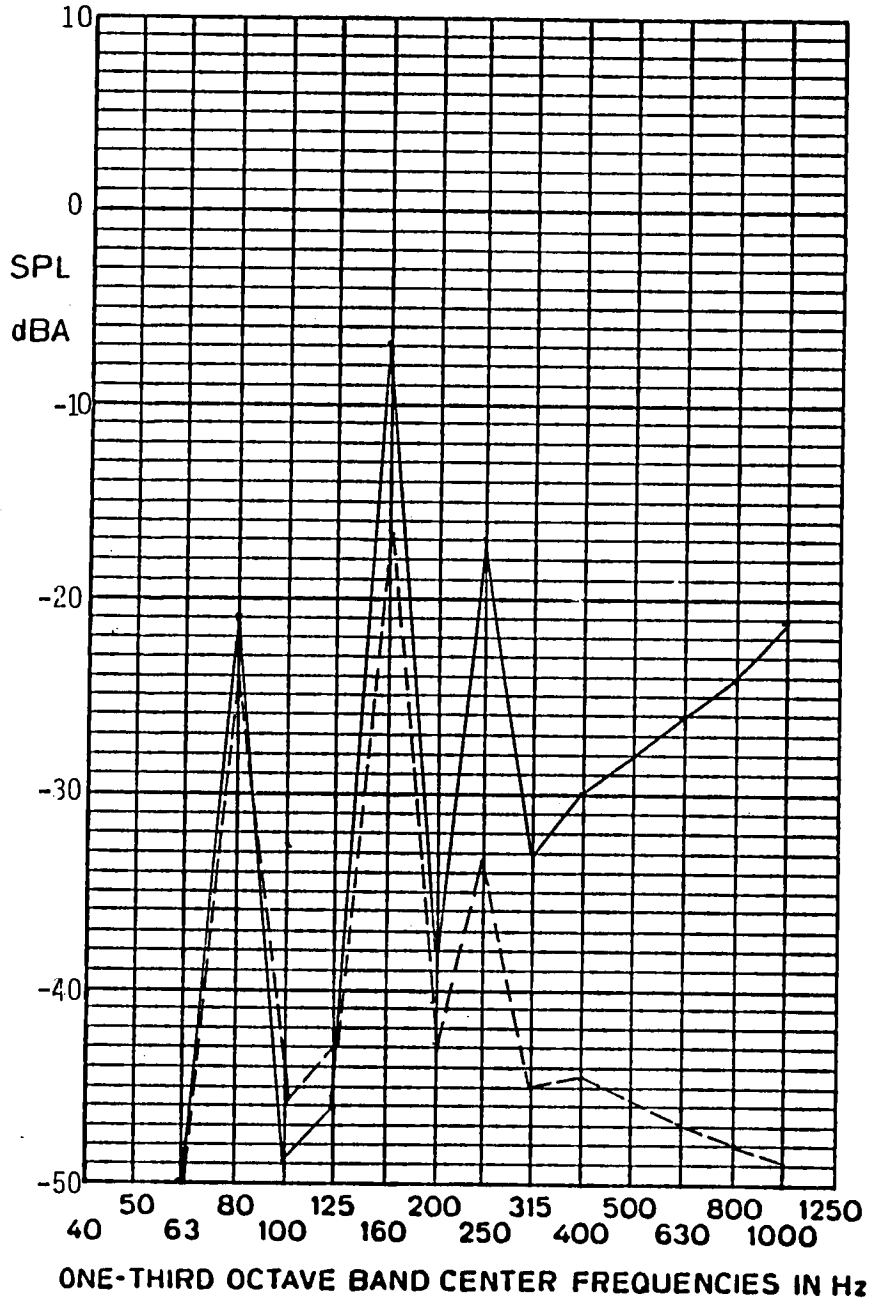

Panel Area = 6 ft^2

Add-on Surface Density = 1.85 lb/ft^2

Added Weight = 11 lbs

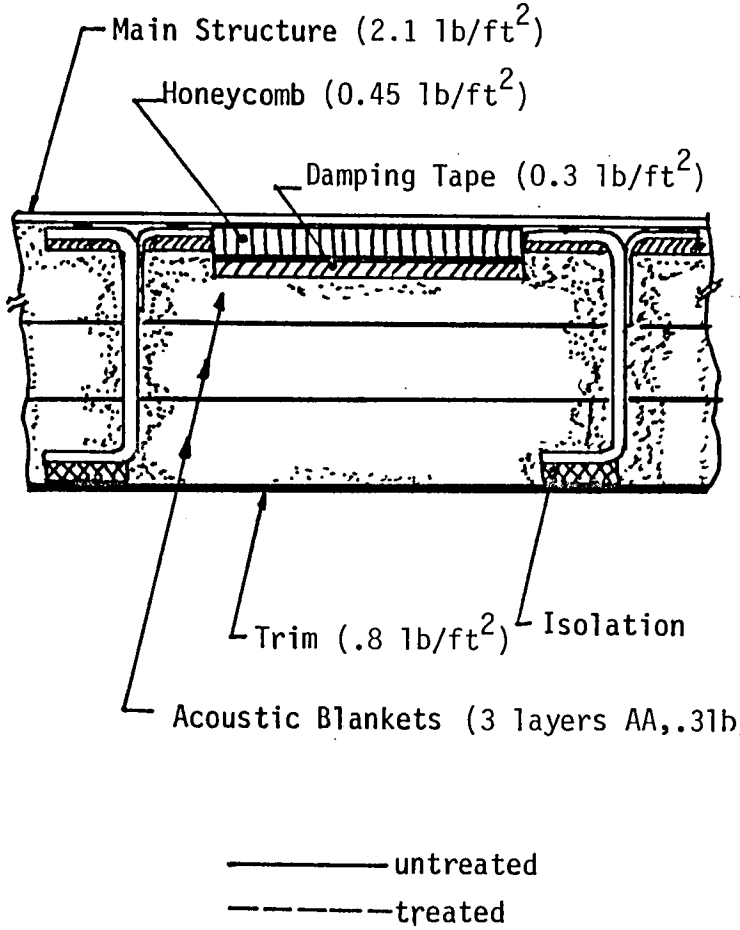

Fig. 26 Transmitted noise for treated and untreated panel (No. 9)

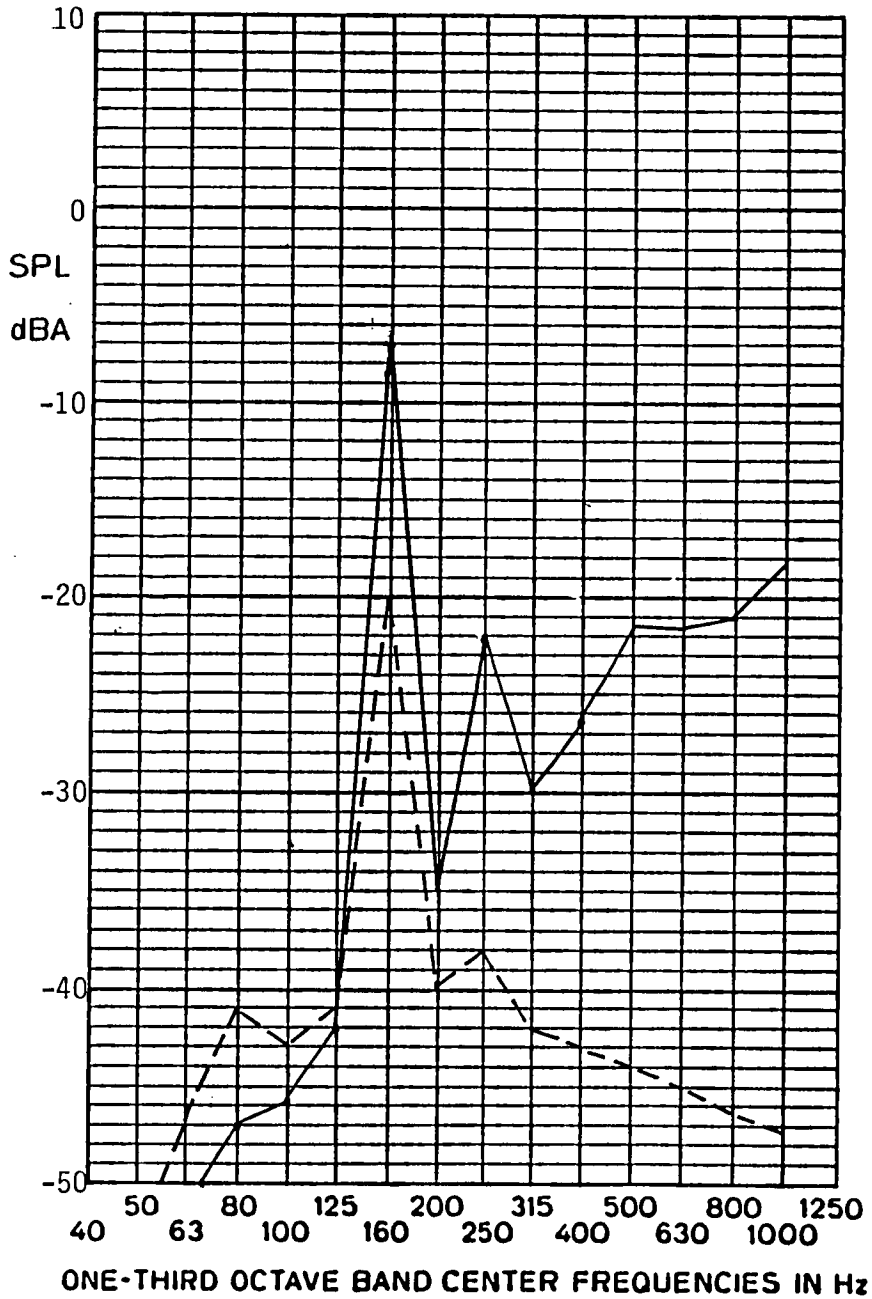

Panel Area = 5 ft^2

Add-on Surface Density = 1.85 lb/ft^2

Added Weight = 9.3 lbs

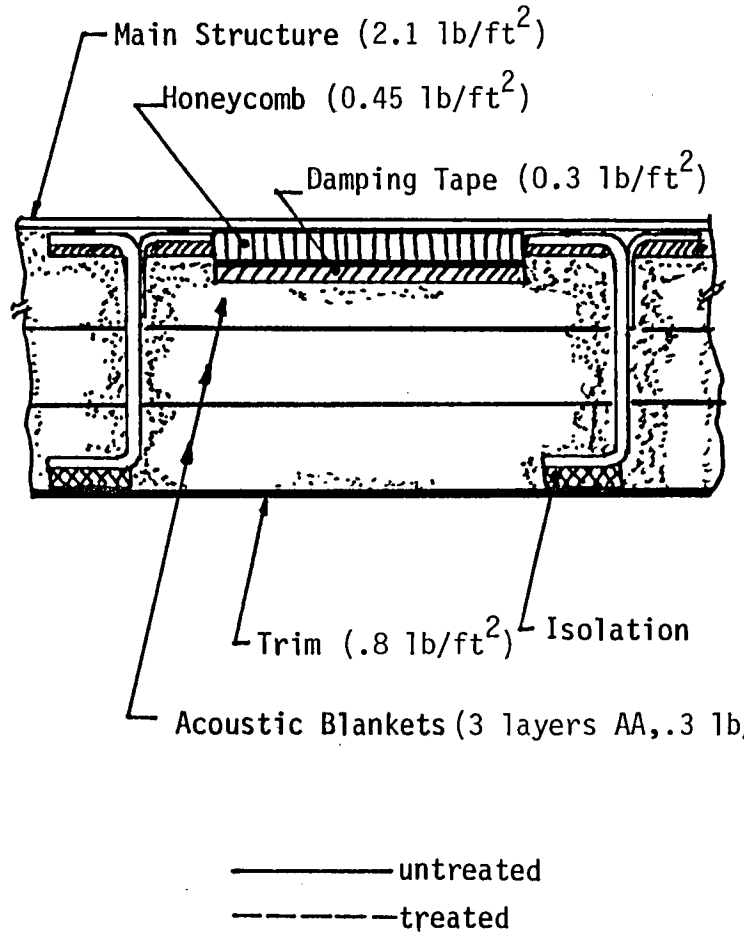

Fig. 27 Transmitted noise for treated and untreated panel (No. 10)

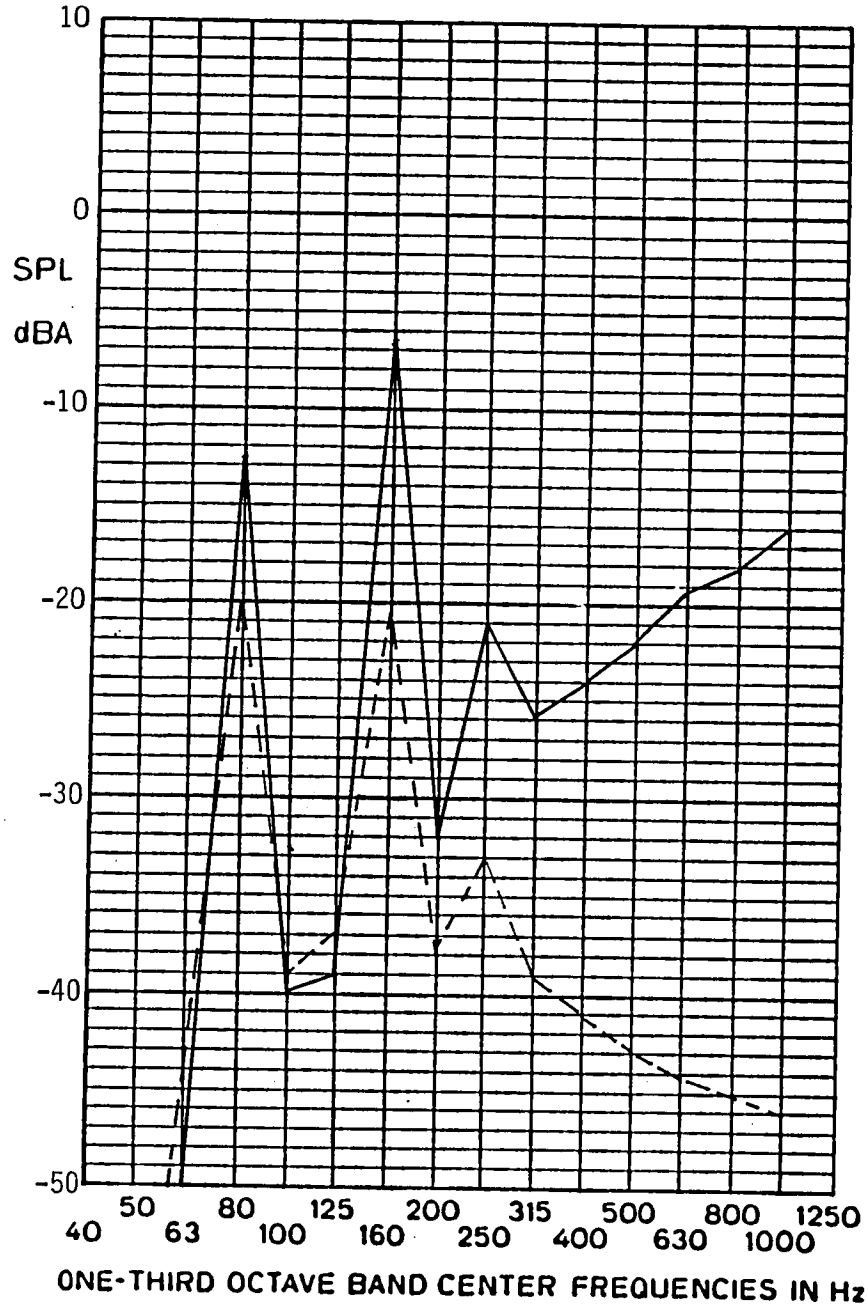

Panel Area = 8.4 ft^2

Add-on Surface Density = 1.85 lb/ft^2

Added Weight = 15.5 lbs

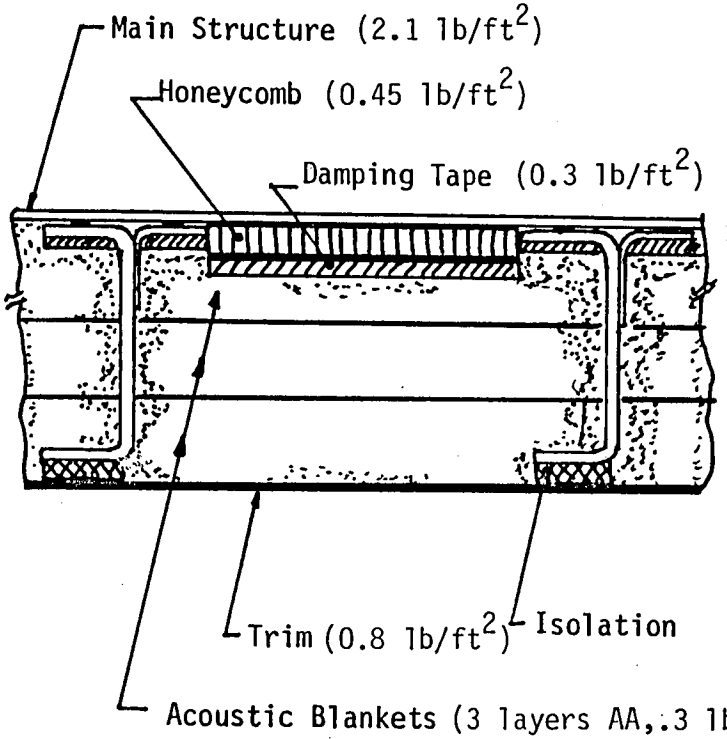

untreated

treated

Fig. 28 Transmitted noise for treated and untreated panel (No. 11)

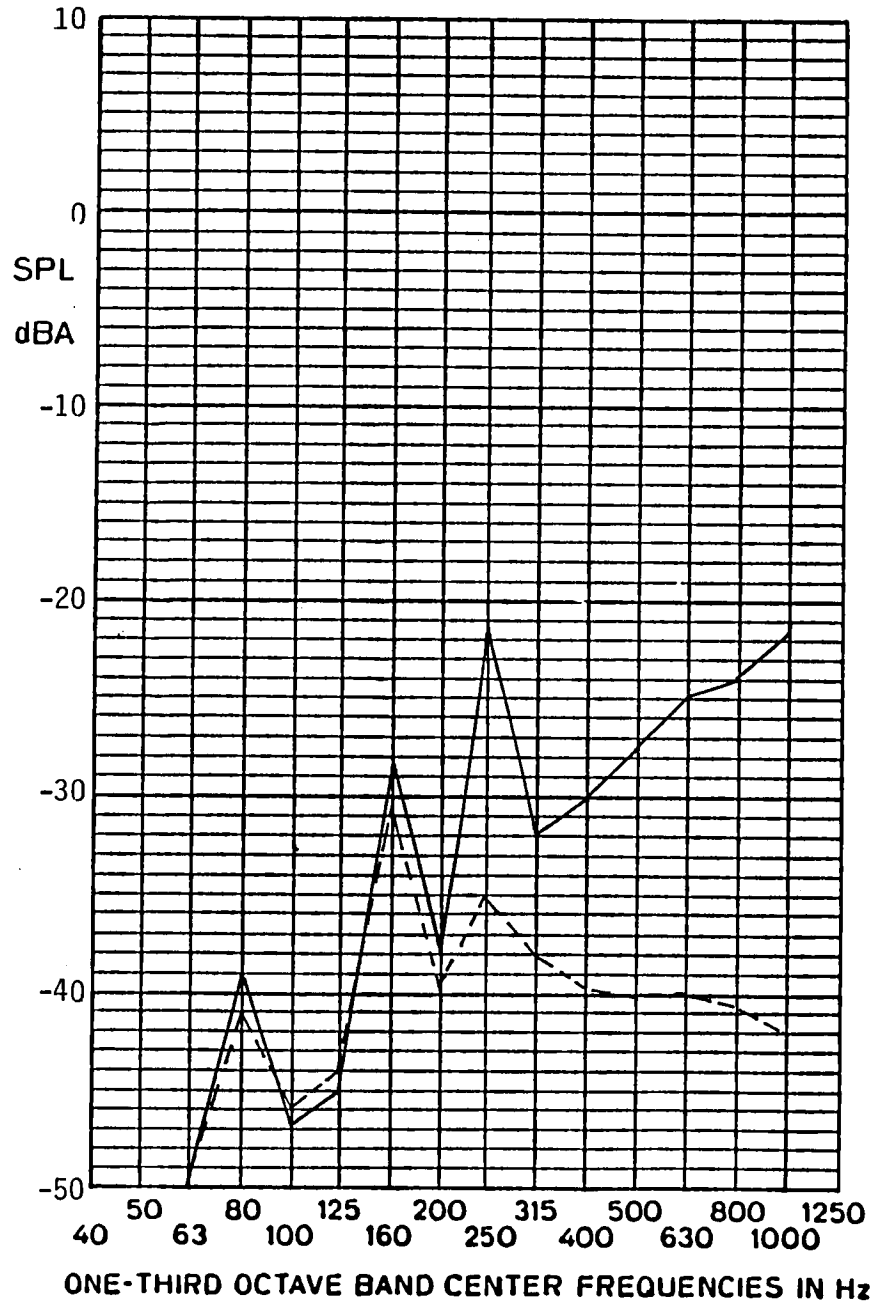

Panel Area = 12 ft^2

Add-on Surface Density = 1 lb/ft^2 (average)

Added Weight = 12 lbs

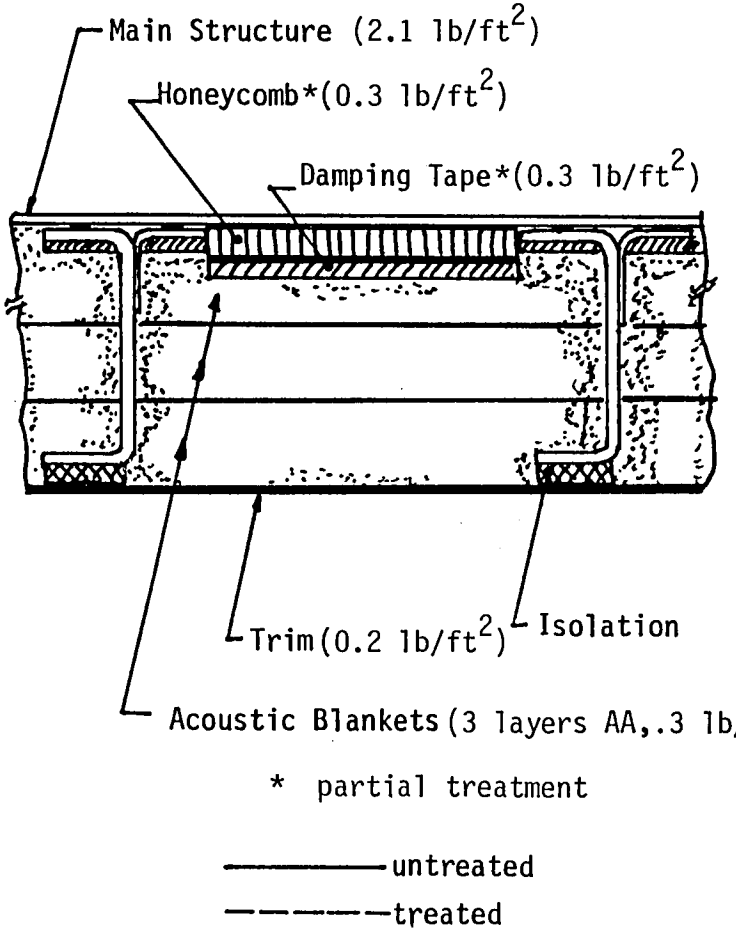

Fig. 29 Transmitted noise for treated and untreated panel (No. 12)

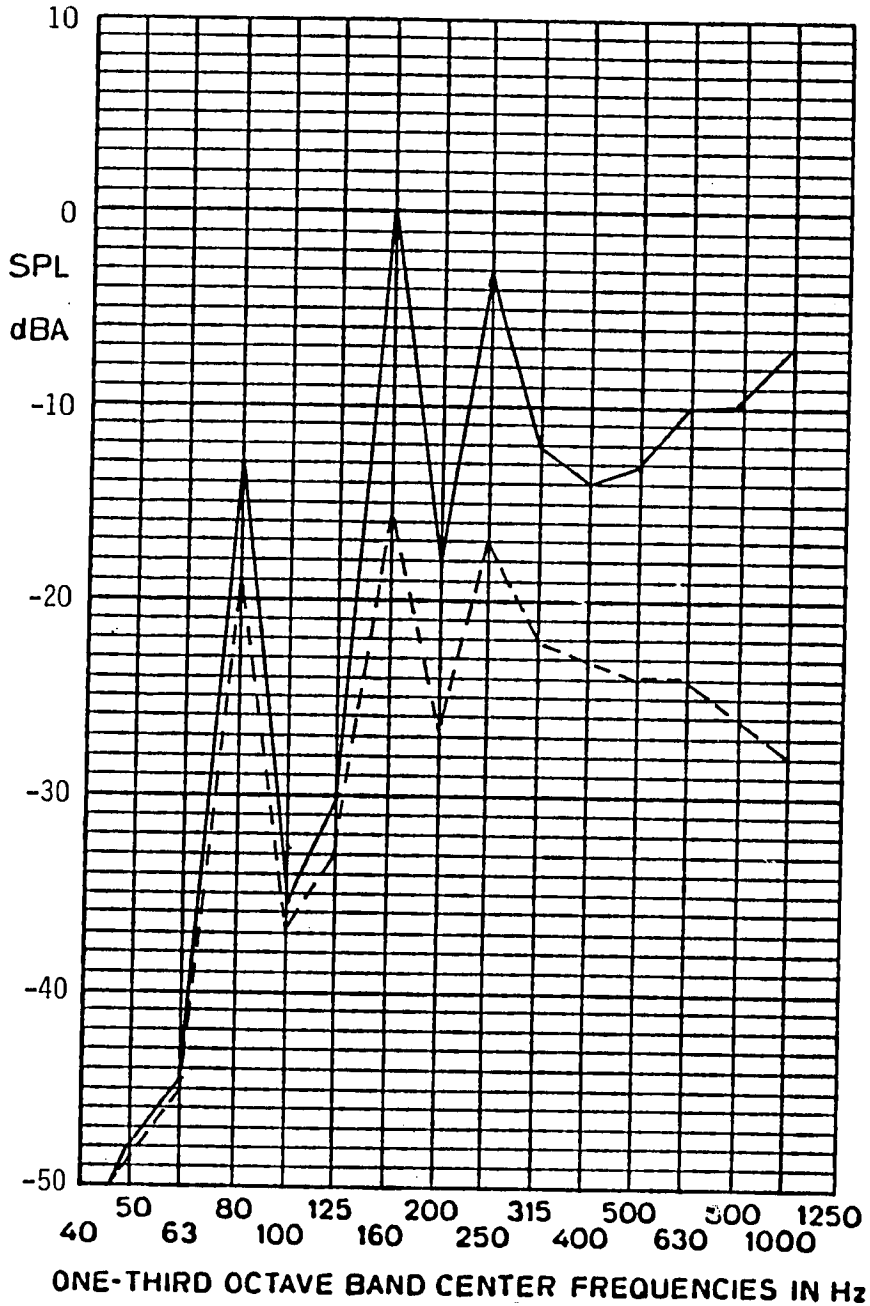

Sidewall Area = 80 ft^2

Added Weight = 110 lbs

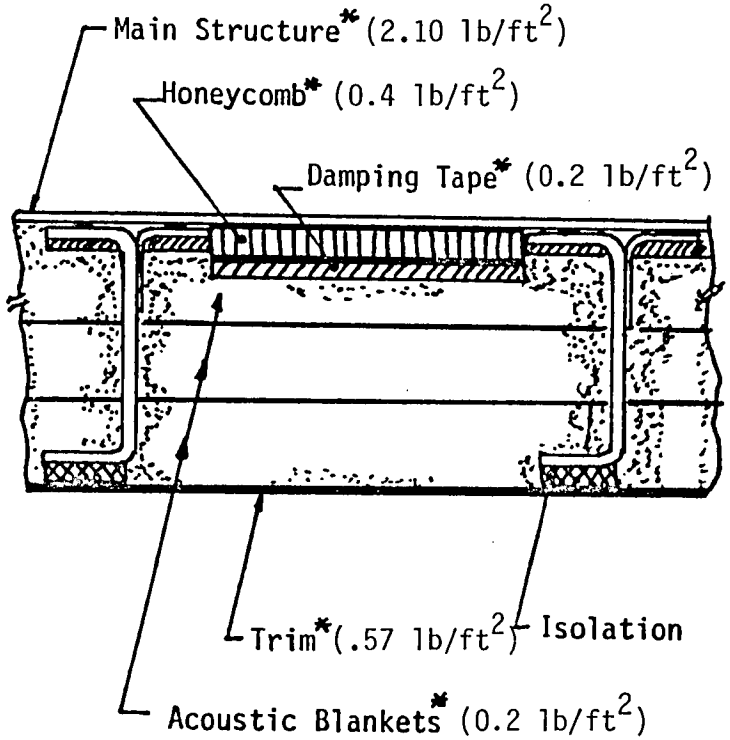

untreated (102 dBA)

treated (87 dBA)

* average values

Fig. 30 Optimized Interior Noise in the Cabin (Sidewall)

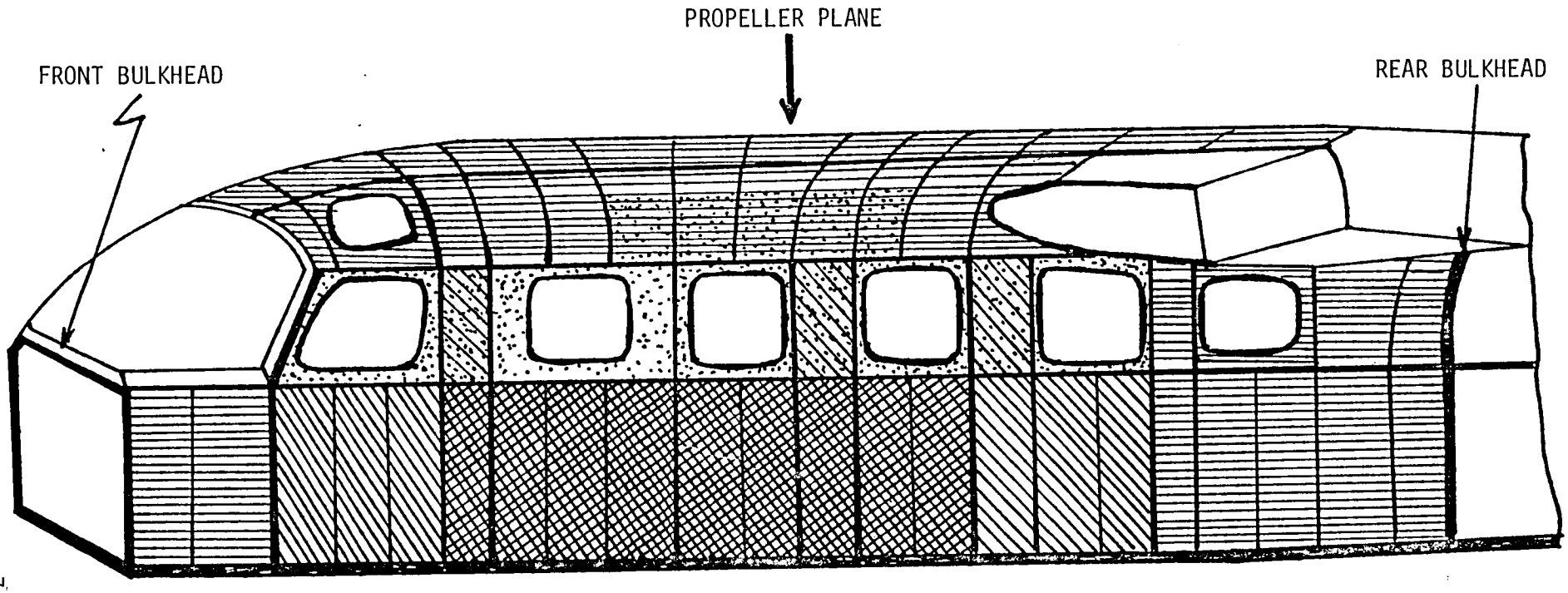

•Honeycomb (0. 45 lb/ft^2)	• Honeycomb (0.3 lb/ft^2)	• Honeycomb (0.3 lb/ft^2)	• Damping Tape (0.15 lb/ft^2)	• Damping Tape 0.25 lb/ft^2)	• Damping Tape 0.25 lb/ft^2)
•Damping Tape (0.25 lb/ft^2)	Damping Tape (0.25 lb/ft^2)	Damping Tape 0.25 lb/ft^2)	3 layers AA$_2$(1") (0.18 lb/ft^2)	3 layers AA$_2$(1") (0.18 lb/ft^2)	3 layers AA$_2$(1") (0.18 lb/ft^2)
•4 layers AA$_2$(1") (0.25 lb/ft^2)	4 layers AA (1") (0.25 lb/ft2)	4 layers (1") (0.18 lb/ft2)	Trim (0.2 lb/ft^2)	Trim (0.4 lb/ft^2)	Trim (1.0 lb/ft^2)
•Trim (0.8 lb/ft^2)	Trim (0.3 lb/ft^2)	Trim (0.3 lb/ft^2)			
Total: 1.75 lb/ft^2	1.1 lb/ft^2	1.03 lb/ft^2	0.53 lb/ft^2	0.83 lb/ft^2	1.43 lb/ft^2

Rear and Front Bulkheads: 3 layers AA (1") + Trim (0.1 lb/ft^2)

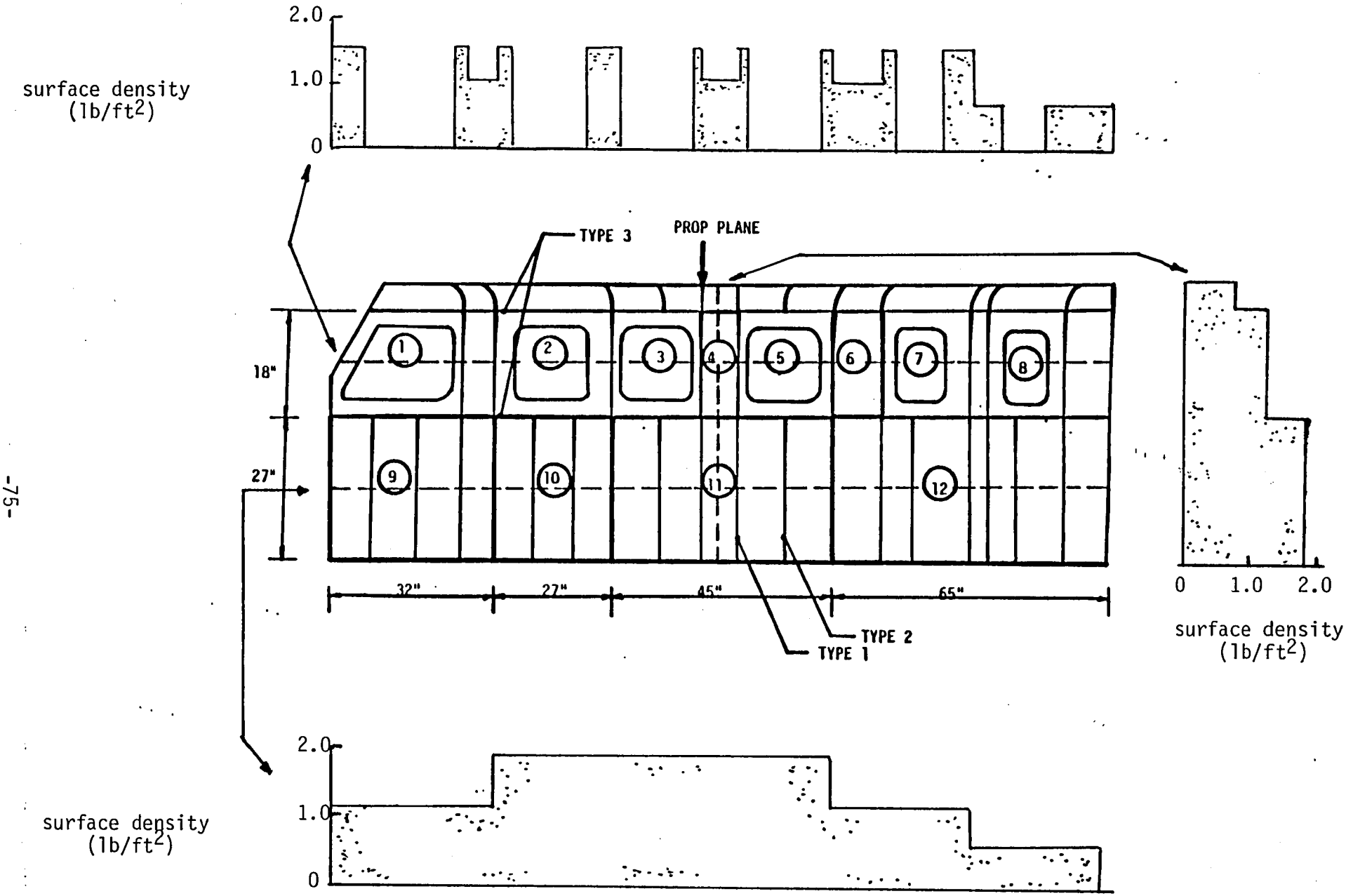

Fig. 32 Distribution of surface density of the add-on treatments

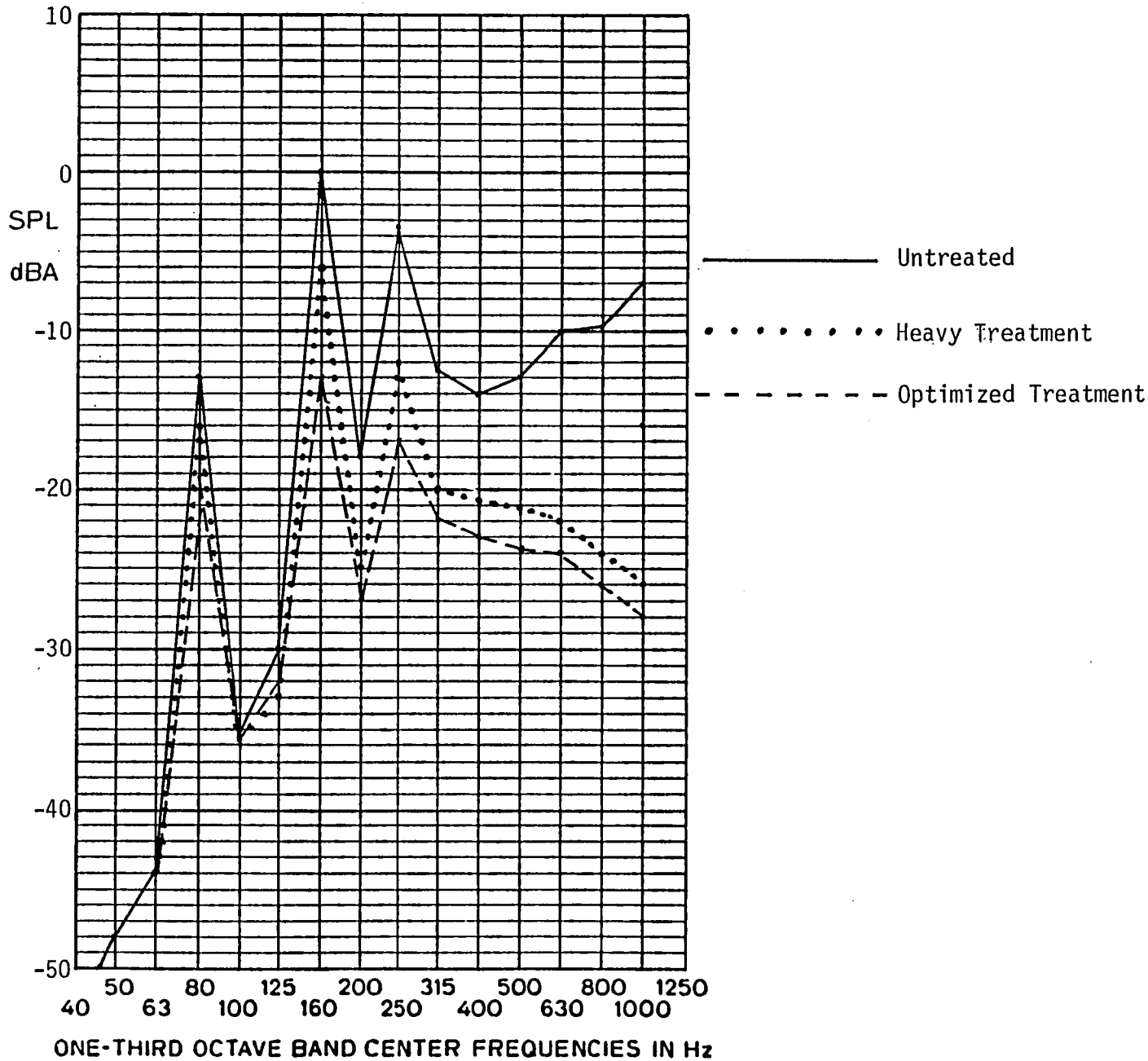

Fig. 33 Transmitted interior noise (sidewall)

APPENDIX A

List of Symbols

A_s = stringer cross-sectional area

A_c = acoustic terms

a = cabin dimensions

a_0, b_0 = distances from x and y axes, respectively, to panel location

b = cabin dimension

C = Saint-Venant constant of uniform torsion

C' = centroid (Fig. 4)

C_{ws} = warping constant of stringer cross-section

c_y, c_z = distances defined in Fig. 4

c = speed of sound

$c_1, \ldots, c_{10}$ = speed of sound in regions 1,....,10, respectively

D = elastic panel stiffness, = $Eh^3/[12(1 - \nu^2)]$

D_h = stiffness of honeycomb panel

D_x, D_y = bending rigidities of skin-stringer panels

d = cabin dimension, also total cavity depth

d_2, d_4, d_6, d_8 = distance between different layers of acoustic treatment

E = total energy (strain + kinetic)

E_s = elastic modulus of the stringer

E_1, E_2 = elastic moduli of the skin and honeycomb panels

f_{mn} = natural frequencies, Hz

H_{mn} = frequency response function of the panel

h = thickness of elastic panel

h_c = honeycomb core thickness

I_x, I_y, I_{xy} = stringer cross-section polar moments of inertia and product of inertia, respectively, about the x and y axes

i,j,m,n = indices

K_{mn} = stiffness matrix of strip element

K_n = banded stiffness matrix

K_2,K_4,K_6,K_8 = compressibility ratios in regions 2, 4, 6 and 8, respectively

L_x,L_y = longitudinal and transverse dimensions of a panel, respectively

M_{mn} = mass matrix of strip element, also generalized mass

M_n = banded mass matrix

m_p = panel mass per unit area

NR = noise reduction

N_X,N_Y = in-plane force resultants

p = acoustic pressure

p_0 = reference acoustic pressure

P_t = transmitted pressure

P_r = reflected pressure

R = average radius of the cabin

R_1 = flow resistivity of the porous material

S = input spectral density

S_p^u = spectral density of untreated structure

S_p^T = spectral density of treated structure

S_{p_i} = spectral density of acoustic pressure

S_w = deflection response spectral density of the panel

S_j^e = cross-spectral density of pressure

S_j = spectral density of external pressure for the j-th panel

SPL = sound pressure levels

t_1,t_2 = thicknesses of skin and honeycomb panel facing, respectively

V = volume of airplane cabin

V_y, V_x = convection velocities of propeller noise corresponding to direction along propeller rotation and perpendicular to it, respectively

x, y, z = spatial coordinates

X_{mn} = structural modes

α = real parts of propagation constant λ

β = imaginary part of propagation constant λ

Δp = pressure differential

$\Delta\omega$ = frequency bandwidth

ΔTL = additional noise transmission losses

δ_n = nodal displacement matrix

ζ_p = structural damping coefficient

ζ_{mn} = structural modal damping coefficients

ζ_T = damping tape coefficient

$\theta_1, \ldots, \theta_{10}$ = incidence angles for different media

η = loss factor of the sidewall

λ = acoustic propagation constant

$\mu_1, \mu_3, \mu_5, \mu_7, \mu_9$ = surface densities of elastic panel, septum barriers and trim panel, respectively

ν = Poisson's ratio

ξ_0 = acoustic damping coefficient

ξ_{ij} = acoustic modal damping coefficients

ρ = air density

$\rho_1, \ldots, \rho_{10}$ = air densities for regions 1,....,10, respectively

$\overline{\rho}$ = material density of the panel

ρ_m = density of acoustic blankets

ρ_f = density of acoustic fibers

ρ_s = material density of stringer

ω = angular frequency

ω_{ij} = acoustic modal frequencies

ω_{mn} = structural modal frequencies

1. Report No.	2. Government Accession No.	3. Recipient's Catalog No.

4. Title and Subtitle	5. Report Date
"Design of Sidewall Treatment for Cabin Noise Control of a Twin Engine Turboprop Aircraft"	December 1983
	6. Performing Organization Code
7. Author(s)	8. Performing Organization Report No.
R. Vaicaitis and M. Slazak	2
	10. Work Unit No.
9. Performing Organization Name and Address	
Modern Analysis Inc. 825 Norgate Drive Ridgewood, NJ 07450	11. Contract or Grant No. NAS1-16117
	13. Type of Report and Period Covered
12. Sponsoring Agency Name and Address	Contractor Report
National Aeronautics and Space Administration (NASA) Washington, DC 20546	14. Sponsoring Agency Code

15. Supplementary Notes

Langley Technical Monitor: Dr. John S. Mixson

16. Abstract

An analytical procedure has been used to predict the noise transmission into the cabin of a twin-engine G/A aircraft. This model was then used to optimize the interior A-weighted noise levels to an average value of about 85 dBA. The surface pressure noise spectral levels were selected utilizing experimental flight data and empirical predictions. The add-on treatments considered in this optimization study include aluminum honeycomb panels, constrained layer damping tape, porous acoustic blankets, acoustic foams, septum barriers and limp trim panels which are isolated from the vibration of the main sidewall structure. To reduce the average noise level in the cabin from about 102 dBA (baseline) to 85 dBA (optimized), the added weight of the noise control treatment is about 2% of the total gross take-off weight of the aircraft.

17. Key Words (Suggested by Author(s))	18. Distribution Statement
Aircraft Interior Noise Propeller Noise Noise Optimization Add-On Treatments	Unclassified. Unlimited Subject Category 71

19. Security Classif. (of this report)	20. Security Classif. (of this page)	21. No. of Pages	22. Price
Unclassified	Unclassified	87	

For sale by the National Technical Information Service, Springfield, Virginia 22161